Phys. Lett. B 862 (2025) 139296

Contents lists available at ScienceDirect

Physics Letters B

journal homepage: www.elsevier.com/locate/physletb

Letter

Search for the Higgs boson decays to a ρ^0, ϕ, or K^{*0} meson and a photon in proton-proton collisions at $\sqrt{s} = 13$ TeV

The CMS Collaboration *

CERN, Geneva, Switzerland

ARTICLE INFO

Editor: M. Doser

Keywords:
CMS
Higgs
Rare decays

ABSTRACT

Three rare decay processes of the Higgs boson to a $\rho(770)^0$, $\phi(1020)$, or $K^*(892)^0$ meson and a photon are searched for using $\sqrt{s} = 13$ TeV proton-proton collision data collected by the CMS experiment at the LHC. Events are selected assuming the mesons decay into a pair of charged pions, a pair of charged kaons, or a charged kaon and pion, respectively. Depending on the Higgs boson production mode, different triggering and reconstruction techniques are adopted. The analyzed data sets correspond to integrated luminosities up to 138 fb^{-1}, depending on the reconstructed final state. After combining various data sets and categories, no significant excess above the background expectations is observed. Upper limits at 95% confidence level on the Higgs boson branching fractions into $\rho(770)^0\gamma$, $\phi(1020)\gamma$, and $K^*(892)^0\gamma$ are determined to be 3.7×10^{-4}, 3.0×10^{-4}, and 3.0×10^{-4}, respectively. In case of the $\rho(770)^0\gamma$ and $\phi(1020)\gamma$ channels, these are the most stringent experimental limits to date.

1. Introduction

In 2012, the ATLAS and CMS experiments at the CERN LHC announced the observation of a new scalar boson [1–3]. Ever since, a multitude of studies have been performed confirming its compatibility with the standard model (SM) Higgs boson (H). In the SM, the Higgs boson interacts with fermion fields via Yukawa-type couplings, which are proportional to the fermion masses. Experimentally, the top quark Yukawa coupling strength is indirectly confirmed through the measurement of the gluon fusion production cross section, as well as by direct measurements of the $t\bar{t}H$ production rate [4,5]. Couplings to the τ lepton and b quark are well established thanks to detailed measurements in the respective Higgs boson decay channels [6–10]. Interactions with c quarks are searched for via the H decay to charm quark jets [11,12] or via signatures involving charmonium [13–15]. Evidence of the Higgs boson coupling to muons has also been established [16].

Direct measurements of the Higgs boson interaction with low-mass quarks (u, d, s) have not yet been possible because of the small predicted couplings, the challenging reconstruction of the final states, and the overwhelming backgrounds induced by quantum chromodynamic (QCD) processes. In order to probe these couplings, decays of the Higgs boson to a light meson plus either a photon or Z boson have been suggested [17]. Upper limits (UL) were obtained for the decays $H \to Z\phi(1020)$ and $H \to Z\rho(770)^0$ [18] by the CMS Collaboration, and for $H \to \rho(770)^0\gamma$, $H \to \phi(1020)\gamma$ [19], $H \to K^*(892)^0\gamma$, $H \to \omega(782)\gamma$ [20] and $H \to D^*(2010)^0\gamma$ [21] by the ATLAS Collaboration. In the analysis presented here we search for exclusive decays of the Higgs boson to a meson and a photon, where the meson is $\rho(770)^0$, $\phi(1020)$, or $K^*(892)^0$. In what follows we will refer to these mesons as ρ^0, ϕ, and K^{*0}, respectively. For the K^{*0} meson the charge-conjugated partner is implied.

The SM prediction for the branching fraction for $\mathcal{B}(H \to \rho^0\gamma)$ and $\mathcal{B}(H \to \phi\gamma)$ are $(1.68 \pm 0.08) \times 10^{-5}$, and $(2.31 \pm 0.11) \times 10^{-6}$, respectively [22]. In both decays, the meson is composed of same-flavor quarks as displayed in the upper half of Fig. 1 for the ϕ meson. The diagram in the upper left shows the Higgs boson directly decaying to a strange quark-antiquark pair while the diagram in the upper right displays a Higgs-boson diphoton Dalitz decay with one off-shell photon, which is dominant in the SM. Beyond-the-SM scenarios with enhanced Higgs boson couplings to light quarks can significantly increase the subdominant contribution and can lead to observable discrepancies that are mostly due to the interference with the dominant diagram [17,23].

The $H \to K^{*0}\gamma$ final state features a flavor-changing neutral current and is therefore strongly suppressed by higher electroweak orders in the SM. Example diagrams are shown in the lower half of Fig. 1. The branching fraction for the $H \to K^{*0}\gamma$ decay is 1.0×10^{-19} [24], and this decay is therefore a powerful probe of possible anomalous flavor-changing Higgs boson couplings [17].

* *E-mail address:* cms-publication-committee-chair@cern.ch.

https://doi.org/10.1016/j.physletb.2025.139296
Received 23 October 2024; Received in revised form 19 January 2025; Accepted 30 January 2025
Available online 3 February 2025

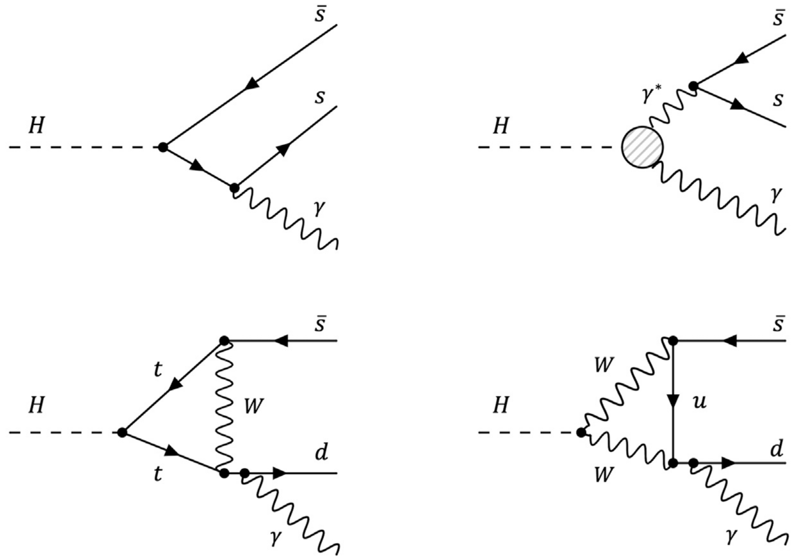

Fig. 1. Feynman diagrams showing the different Higgs boson decay mechanisms into a photon and a light meson (upper: ϕ meson; lower: K^{*0} meson). The hatched circle in the upper right diagram denotes the off-shell $H \to \gamma\gamma^*$ amplitude, which in the SM arises first at one-loop order.

For our search, we analyze proton-proton (pp) collision data at $\sqrt{s} = 13$ TeV, collected with the CMS detector at the LHC. Events are separated into mutually exclusive categories targeting the main production modes of the Higgs boson at the LHC, namely gluon fusion (ggH), vector boson fusion (VBF), and associated production with a vector boson (VH, V = Z, W). The VH events contain leptonic decays of the vector bosons, $W \to \ell\nu$ and $Z \to \ell\ell$, where $\ell = e, \mu$. The VH category also includes contributions from events where Higgs boson production occurs in association with top quarks ($t\bar{t}H$), with leptonic decays from the resulting W bosons. To reconstruct Higgs boson candidates, photons are combined with meson candidates, identified via their decays $\rho^0 \to \pi^+\pi^-$, $\phi \to K^+K^-$ and $K^{*0} \to K^+\pi^-$.

Tabulated results are provided in the HEPData record for this analysis [25].

2. The CMS detector

The central feature of the CMS apparatus is a superconducting solenoid of 6 m internal diameter, providing a magnetic field of 3.8 T. Within the solenoid volume are a silicon pixel and strip tracker, a lead tungstate crystal electromagnetic calorimeter (ECAL), and a brass and scintillator hadron calorimeter, each composed of a barrel and two endcap sections. A silicon strip preshower detector improves energy measurements in the forward region. Forward calorimeters extend the pseudorapidity (η) coverage provided by the barrel and endcap detectors. Muons are reconstructed in gas-ionization detectors embedded in the steel flux-return yoke outside the solenoid.

The silicon tracker measures charged particles within the pseudorapidity range $|\eta| < 2.5$. It consists of 1856 silicon pixel and 15 148 silicon strip detector modules. The silicon pixel detector modules are arranged in four layers. In 2016, data were taken with a different detector configuration; at that time there were 1440 silicon pixel detector modules arranged in three layers. The relative p_T resolution for nonisolated particles in the barrel region, $|\eta| < 1.4$, is $\approx 1\%$ independent of p_T in the range 1-10 GeV, increases with p_T above 10 GeV, reaching $\approx 2\%$ at 50 GeV and $\approx 4\%$ at 100 GeV [26].

Muons are measured in the pseudorapidity range $|\eta| < 2.4$, with detection planes made using three technologies: drift tubes, cathode strip chambers, and resistive-plate chambers. The single muon trigger efficiency exceeds 90% over the full η range, and the efficiency to reconstruct and identify muons offline is greater than 96%. Matching muons to tracks measured in the silicon tracker results in a relative p_T resolution, for muons with p_T up to 100 GeV, of 1% in the barrel and 3% in the endcaps [27].

The electron momentum is estimated by combining the energy measurement in the ECAL with the momentum measurement in the tracker. The momentum resolution for electrons with $p_T \approx 45$ GeV from $Z \to ee$ decays ranges from 1.6 to 5%. It tends to be better in the barrel region than in the endcaps, and also depends on the bremsstrahlung energy emitted by the electron as it traverses the material in front of the ECAL [28].

The energy of photons is obtained from the ECAL energy depositions in a supercluster, combining deposits from the photon and the conversions, produced by the tracker material upstream of the ECAL detector. The energy resolution for photons varies between 8 and 3% in the p_T range of 20 to 100 GeV [28].

Events of interest are selected using a two-tiered trigger system [29]. The first level, composed of custom hardware processors, uses information from the calorimeters and muon detectors to select events at a rate of around 100 kHz within a fixed latency of 4 μs [30]. The second level, known as the high-level trigger, consists of a farm of processors running a version of the full event reconstruction software optimized for fast processing, and reduces the event rate to around 1 kHz before data storage [31].

A more detailed description of the CMS detector, together with a definition of the coordinate system used and the relevant kinematic variables, can be found in Ref. [32].

3. Simulated samples

Samples of simulated Higgs boson events, produced via ggH, VBF, $t\bar{t}H$, WH, and ZH, are generated at next-to-leading order (NLO) in QCD using POWHEG 2.0, with improved accuracy where available [33–38]. The signal yields are normalized to the theoretical cross sections. The ggH cross section is calculated at next-to-next-to-NLO in QCD and at NLO in electroweak accuracy, while those for the other production modes are calculated at next-to-NLO in QCD and at NLO in electroweak accuracy [39]. The decay $\rho^0 \to \pi^+\pi^-$ has a branching fraction of $\approx 100\%$, while the decay $\phi \to K^+K^-$ has a branching fraction of $(49.1 \pm 0.5)\%$. For the decay $K^{*0} \to K\pi$, the branching fraction is close to 100%, with two-thirds of these decays involving a charged kaon and a charged pion [40].

Simulated samples are utilized to measure data-to-simulation correction factors for the object identification and trigger selection efficiency; these simulations are also employed to optimize the event selections within each category. The related SM processes are: γ, $W \to \ell\nu$, and Drell–Yan $Z \to \ell\ell$ production in association with jets, as well as $t\bar{t}$, $W\gamma$, and $Z\gamma$ production. These samples are generated at leading order (LO) using MADGRAPH5_aMC@NLO 2.6.5 with MLM parton matching [41], MADGRAPH5_aMC@NLO 2.6.5 at NLO, with FxFx matching [42] or POWHEG program. The NNPDF3.1 parton distribution functions (PDFs) [43] at next-to-NLO order are used for all samples.

All generated samples are interfaced with PYTHIA 8.212 [44] to model parton showering and hadronization. The description of the underlying event is provided by the CP5 tune [45]. For the signal samples the decays $H \to \rho^0\gamma$, $H \to \phi\gamma$, or $H \to K^{*0}\gamma$ are also modeled using PYTHIA. With the Higgs boson being a scalar particle, angular momentum conservation enforces fully transverse spin alignment of the outgoing vector meson, but PYTHIA simulates unpolarized decay products. To account for this effect, signal events are weighted at generator level by a factor proportional to $\sin^2\theta$, where θ is the angle between the direction of the positive kaon or pion in the meson rest frame and a polarization axis defined as the meson flight direction in the Higgs boson rest frame; the polarization axis can be effectively approximated, in the present case, with the meson flight direction measured in the laboratory, given the smallness of the meson masses with respect to the Higgs boson mass [46]. A validation of this reweighting has been performed using EVTGEN [47].

Additional inelastic pp collisions in each bunch crossing, referred to as pileup (PU), are generated with PYTHIA and are added to all simulated events in accordance with the measured PU distribution. All generated events are processed through a GEANT4-based [48] simulation of the CMS detector before being reconstructed with the same version of the CMS event reconstruction software used for data. Detector conditions corresponding to the different data-taking periods in years 2016, 2017, and 2018 are simulated separately.

4. Event reconstruction

The final-state particles of pp collisions are reconstructed with a particle-flow (PF) algorithm [49], which combines information from all subdetectors to reconstruct individual particle candidates (PF candidates). These particle candidates are classified as muons, electrons, photons, charged and neutral hadrons.

The primary vertex (PV) is taken to be the vertex corresponding to the hardest scattering in the event, evaluated using tracking information alone, as described in Section 9.4.1 of Ref. [50]. All other collisions in the event are considered to have originated from PU. The candidate muons, electrons, and charged-hadron tracks used in the search presented in this paper are all required to originate from the PV.

Candidate photons from the particle-flow algorithm must satisfy a tight (medium) identification multivariate analysis (MVA) criterion corresponding to a true-photon efficiency of 80% (90%) [28], depending on the event selection described in Section 5. Discriminating variables include photon kinematic observables and ECAL-to-preshower energy ratios in the endcaps, variables related to electromagnetic shower shape and width, and the isolation of the photon candidate. The isolation variable is computed either considering only tracks or all PF candidates in a cone within $\Delta R = 0.4$ from the cluster centroid, where $\Delta R = \sqrt{(\Delta\eta)^2 + (\Delta\phi)^2}$ and $\Delta\eta$ and $\Delta\phi$ are differences in pseudorapidity and azimuthal angle, respectively. Vetoes are applied in order to reject electron candidates and photons that converted into an electron-positron pair [28]. Corrections on photon energy scale, resolution, and identification efficiency, derived from $Z \to ee$ events [28] using the "tag-and-probe" (TnP) method [51], are applied to simulated events.

Muons are required to satisfy identification and isolation criteria with an average selection efficiency of about 95%. An isolation variable (I^{μ}_{rel}) for muons is determined by summing the p_T of all PF candidates within a cone of radius $\Delta R = 0.4$ around the direction of the candidate muon and is corrected for the contribution of neutral particles from PU interactions [52]. Factors correcting for the identification efficiency of muons have been computed using the TnP method.

To reduce contamination from incorrectly reconstructed particles, candidate electrons are required to pass a tight (medium) MVA electron identification discriminant corresponding to an efficiency of 80% (90%), depending on the event selection. This discriminant [28] combines information about the quality of the tracks, the shower shape, kinematic quantities, and hadronic activity in the vicinity of the reconstructed electron. Electron energy scale and resolution corrections, derived from $Z \to ee$ events [28], are applied to simulated events. The TnP method is also used to determine correction factors of the electron identification efficiency [27,28].

Jets are reconstructed from PF candidates using the anti-k_T clustering algorithm [53,54] with a distance parameter of 0.4. To mitigate the effect of PU, charged hadrons that do not arise from the PV are removed from the clustering. In addition to jet identification criteria, PU rejection criteria are used to reduce the contamination of jets with $p_T^j < 50\,\text{GeV}$ initiated by PU interactions [55]. Differences in jet energy scale and resolution between data and simulation are corrected for, as described in Ref. [56].

The meson candidates are identified using tracks reconstructed in the tracking detector. The tracks are required to originate from the PV and to satisfy the "high purity" reconstruction requirements. These requirements are based on the number of tracker layers with reconstructed hits, the track fit quality, and the values of the impact parameters relative to their uncertainties [26]. A ρ^0, ϕ or K^{*0} meson candidate, denoted generically as "M", is reconstructed as a pair of oppositely-charged tracks, one with $p_T > 20\,\text{GeV}$ and the other with $p_T > 5\,\text{GeV}$; both within $|\eta| < 2.5$. The pseudorapidity of the meson is restricted to match the trigger requirements, described in Section 5. The meson decay vertex is determined with a kinematic vertex-constrained fit [57] and track momenta are recalculated accordingly. An isolation variable of the meson candidate is determined using PF candidate transverse momenta as:

$$I^{\text{ch}}(\text{M}) = \frac{p_T^{\text{M}}}{p_T^{\text{M}} + \sum_{\text{ch}} |p_T^{\text{ch}}|},$$
$$I^{\text{neu}}(\text{M}) = \frac{p_T^{\text{M}}}{p_T^{\text{M}} + \sum_{\text{neu}} |p_T^{\text{neu}}|}, \quad (1)$$

where $\sum_{\text{ch}} |p_T^{\text{ch}}|$ and $\sum_{\text{neu}} |p_T^{\text{neu}}|$ are, respectively, the p_T sums of tracks and neutral particle candidates in a cone of radius $\Delta R = 0.3$ around the direction of the two-track system. Only tracks with $p_T > 0.9\,\text{GeV}$ associated with the meson vertex, excluding the candidates defining the meson, and only neutral candidates with $p_T > 0.5\,\text{GeV}$, are retained in the isolation variable calculation. Data-to-simulation correction factors accounting for differences in track- and neutral particles based isolation variables are derived from events with two oppositely-charged muons using the following TnP method. After identifying a high-quality muon, isolation variables are computed from the activity around a second candidate muon in the event, satisfying looser criteria, which serves as a proxy for the candidate meson. The efficiency of the isolation requirement is extracted fom a simultaneous Z+background fit to the dimuon mass distribution for events passing or failing the isolation requirement. This efficiency is compared to the ditrack isolation efficiency estimated from the signal samples to derive corrections, which amount to values around 1% depending on p_T^{μ}. A systematic uncertainty arising from using a muon as a proxy for a meson is applied and detailed in Section 8.

It is required that the track-pair mass, under the appropriate charged-pion or charged-kaon mass hypotheses for the tracks, is consistent with the corresponding nominal meson mass. The experimental resolution ranges from approximately 3 MeV for m_{KK} to 8 MeV for $m_{\pi\pi}$. Events are selected if the mass of the ditrack system is within the ranges defined in Table 1. In the K^{*0} case, if both the $K^+\pi^-$ and the $K^-\pi^+$ candidates fall in the mass interval, the one with the mass closest to the nominal K^{*0} mass is chosen. No attempt is made to make these

Table 1
Mass requirements imposed on the ditrack system for signal and sideband regions.

meson decay	lower boundary (GeV)	signal region (GeV)	upper boundary (GeV)
$\rho^0 \to \pi^+\pi^-$	0.55	0.62 – 0.92	1.00
$\phi \to K^+K^-$	1.000	1.008 – 1.032	1.042
$K^{*0} \to K^+\pi^-$	0.80	0.84 – 0.94	1.00

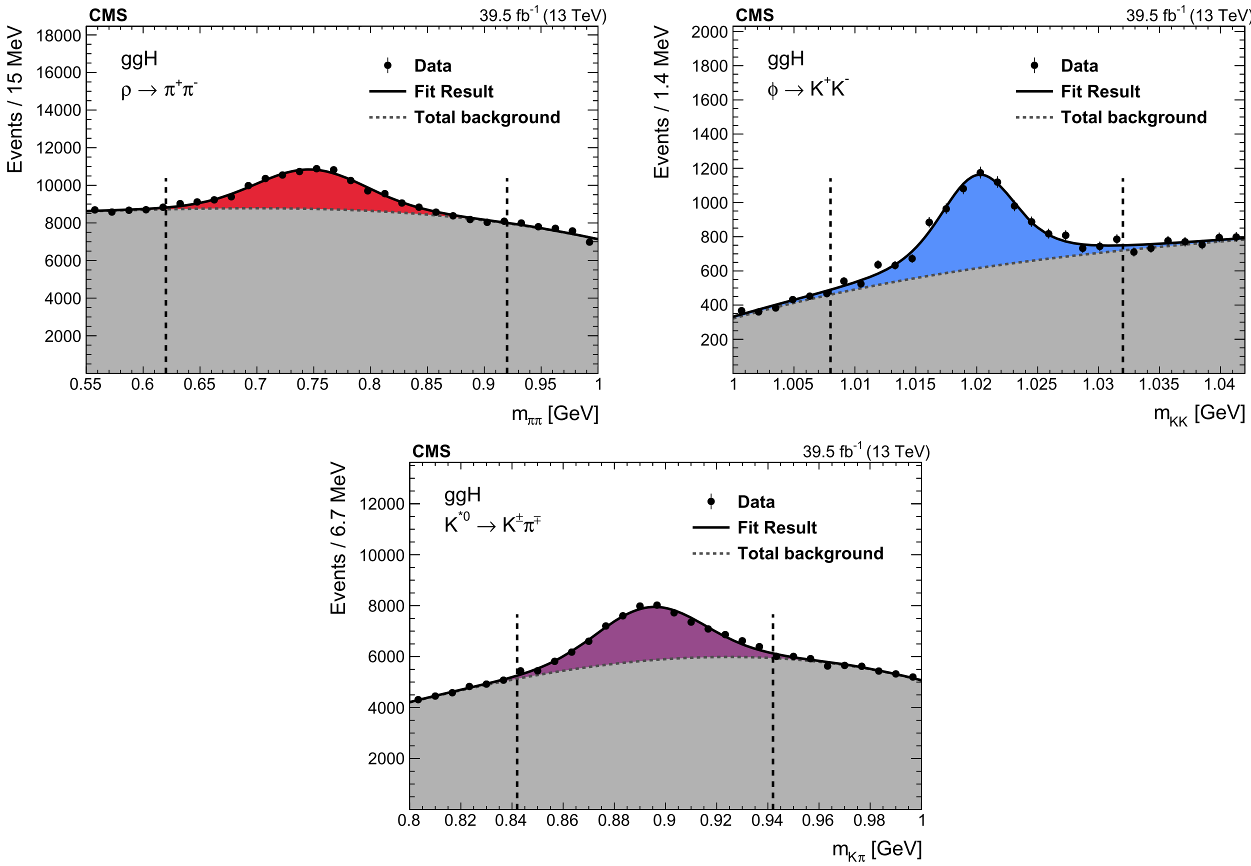

Fig. 2. Track pair invariant mass distributions in selected data events, for the ggH category of the analysis, for the $\rho^0\gamma$ (upper left), $\phi\gamma$ (upper right), and $K^{*0}\gamma$ (lower) decays. The vertical dashed lines represent the signal mass region borders.

selections mutually exclusive. Moreover, if more than one meson candidate in the relevant mass intervals are found in the same event, only the one with the largest p_T is retained in the corresponding search. The mass intervals located on either side of the signal mass regions form a *sideband region*, as defined in Table 1. The sideband region is used for training an MVA discriminator in the ggH category, and to validate another MVA discriminator used in the VBF category, as described in Section 6. The distributions of the ditrack system mass in the three decay channels are shown in Fig. 2, exhibiting a visible resonance peak at the mass of the meson. The meson peaks are fitted with a Voigtian function and the background with a third-order Chebychev polynomial. Fig. 2 provides a qualitative illustration of the meson selection in the ggH category.

5. Event selection

In the following, four analyses categories that target $t\bar{t}H$, VH, VBF, and ggH processes are discussed. The corresponding event selection criteria are summarized in Table 2. In the ggH and VBF categories, the background is mostly composed of γ+jet and multijet events, which occur at rates many orders of magnitude larger than that of Higgs boson production. Main backgrounds in the VH category are $W \to \ell\nu$, and Drell–Yan $Z \to \ell\ell$ production in association with jets, as well as $t\bar{t}$, $W\gamma$, and $Z\gamma$ events.

5.1. VH category

The VH category targets production of a Higgs boson in association with a heavy vector boson. However signal events selected under VH category also include $t\bar{t}H$ events where one or both W bosons from top quark decays yield leptons, accounting for approximately 30% of the event statistics in this category. Trigger selection is based on single- or double-lepton requirements, where the single-muon (electron) lowest p_T thresholds vary between 24 and 27 GeV (27 and 32 GeV), depending on the data-taking period, while the double-muon (electron) lowest p_T thresholds are 17 and 8 GeV (23 and 12 GeV). Triggers requiring a muon with $p_T^{\mu} > 17$ GeV and a photon with $p_T^{\gamma} > 30$ GeV complement the selection. These triggers were active for the full data-taking periods in years 2016, 2017, and 2018 corresponding to 138 fb^{-1}.

In the $W \to \ell\nu$ decay channel, events are retained if they contain a muon with $p_T^{\mu} > 20$ GeV and $I_{rel}^{\mu} < 0.15$, or an electron with $p_T^{e} > 30$ GeV, where both must satisfy tight identification criteria. In the $Z \to \ell\ell$ decay channel, two muons are required with $p_T^{\mu} > 20$ and 10 GeV, and $I_{rel}^{\mu} <$ 0.25, or two electrons with $p_T^{e} > 25$ and 15 GeV, where both must satisfy tight identification criteria. All electrons (muons) must be within $|\eta| <$

2.5 (2.4). The ZH category includes events with two opposite-charge and same-flavor leptons if they satisfy $|M_{\ell\ell} - M_Z| < 15\,\text{GeV}$.

Events are required to contain photons with $p_T^\gamma > 40\,\text{GeV}$, $|\eta^\gamma| < 2.5$ and satisfying medium identification criteria. Meson candidates must have $p_T^M > 40\,\text{GeV}$ and $I^{ch}(M) > 0.8$. In the single-muon final state, it is required that $\Delta R(\mu, M) > 0.5$. In the single-electron final state, events with electron-photon pairs consistent with the Z boson decays are vetoed by requiring $|M_{e\gamma} - M_Z| > 10\,\text{GeV}$ to reduce background from electrons misidentified as photons. In the dilepton final state, an additional requirement is imposed on the mass of the dilepton-γ system, $M_{\ell\ell\gamma} > 96\,\text{GeV}$ in order to reduce the impact of final-state radiation (FSR). A lepton veto is applied in the other categories described below to ensure they are mutually exclusive.

5.2. High-p_T^γ VBF category

The high-p_T^γ VBF category targets VBF events with a high-energy photon. During the data taking these events are selected by a trigger requiring a photon with $p_T^\gamma > 75\,\text{GeV}$, in the ECAL barrel region ($|\eta^\gamma| < 1.4$), and a pair of jets with large invariant mass ($M_{jj} > 400\,\text{GeV}$) and large separation in pseudorapidity ($|\Delta\eta_{jj}| > 3$). The threshold values were adjusted throughout the data-taking years. This trigger was used for part of 2016 (28.2 fb^{-1}) and part of 2017 (7.7 fb^{-1}), and for all of 2018 (63.7 fb^{-1}).

Events are required to contain photons with $p_T^\gamma > 75\,\text{GeV}$, that satisfy medium photon identification criteria. Photons in the ECAL endcaps are not considered because the trigger was limited to the ECAL barrel region. Events must also include meson candidates with $I^{ch}(M) > 0.9$ and $p_T^M > 30\,\text{GeV}$. In addition, two jets not overlapping with the $H \to M\gamma$ signal candidate are required, which must satisfy $p_T^j > 40\,\text{GeV}$, $M_{jj} > 400\,\text{GeV}$, and $|\Delta\eta_{jj}| > 3$.

5.3. Low-p_T^γ VBF category

Since the VBF trigger is ineffective for low-p_T photons, we adopt a trigger strategy introduced in 2018 (39.5 fb^{-1}), only based on the Higgs decay products. This trigger selects a photon and a jet each with $p_T > 35\,\text{GeV}$. In addition, the jet must be compatible with a single, isolated ditrack system. The photon selection is based on the ratio of the HCAL and ECAL cluster energies, shower-shape parameters, and isolation computed from ECAL and HCAL energy deposits and tracker information, in a cone of $\Delta R = 0.4$ around the candidate photon. Utilizing the similarity among the tau lepton hadronic decay and the meson signature, trigger requirements on the ditrack system follow those of τ reconstruction. Final states with two tracks and no π^0 mesons are selected requiring the tight working point for τ identification and isolation [58]. Finally the photon-jet system must satisfy $\Delta R_{j,\gamma} > 0.3$ and $M_{j,\gamma} > 30\,\text{GeV}$. The trigger efficiency for the Higgs boson signal is around 55% with respect to the offline selection.

The efficiency of the photon and τ-like jet reconstruction at trigger level was studied by factorizing the trigger efficiency into the photon and τ-like jet parts, and using two dedicated triggers. These triggers require a muon with $p_T^\mu > 24\,\text{GeV}$, as well as a photon or a τ-like jet with the same requirements as the signal. In data and simulated events, a $Z \to \mu\mu$ boson candidate and a photon or a meson candidate are reconstructed, where one of the two candidate muons from the Z boson matches the muon trigger objects. The meson (photon) trigger efficiency for data and simulation is determined by measuring the fraction of the Z-plus-meson (-photon) events that also pass the dedicated trigger requirement. The photon trigger efficiency is determined using events where the photon-plus-dimuon mass is compatible with that of the Z boson.

Selected events are required to contain at least one photon with $38 < p_T^\gamma < 75\,\text{GeV}$, $|\eta^\gamma| < 2.1$ that passes the medium (tight) identification criteria in the ECAL barrel (endcap). Events are required to have at least one meson candidate with $p_T^M > 38\,\text{GeV}$ and $I^{ch}(M) > 0.9$. To confirm the VBF nature of the category, we require a pair of jets with $p_T^j > 30$ and 20 GeV, $M_{jj} > 300\,\text{GeV}$, and $|\Delta\eta_{jj}| > 3$, where the jets do not overlap with the $H \to M\gamma$ signal candidates. In the following, jets satisfying these criteria are referred to as VBF-like jets.

5.4. ggH category

The ggH category includes events selected by the same trigger as the low-p_T^γ VBF category. After a VBF-like jets veto is applied and the overlap with other categories is removed, events are required to contain photons with $p_T^\gamma > 38\,\text{GeV}$, $|\eta^\gamma| < 2.5$ and passing the tight identification criteria. Since the mesons from the Higgs boson decays have a large momentum, their secondary decay products are expected to be collimated, and hence have a jet-like signature. As meson candidate tracks, we consider the two leading-p_T charged constituents of a jet which satisfies basic jet requirements [59], and that lie in a cone with $\Delta R = 0.07$ between the tracks direction, thus strongly reducing track combinations. Candidate mesons with $p_T^M > 38\,\text{GeV}$, $I^{ch}(M) > 0.9$ and $I^{neu}(M) > 0.8$ are retained. This category includes approximately 4% of VBF signal events.

6. Multivariate analysis selection

An analysis-specific MVA selection, based on a boosted decision tree (BDT) algorithm, has been developed to improve the signal-to-background ratio in the ggH, VBF low-p_T^γ, and VBF high-p_T^γ categories. The BDT classifiers use gradient boosting [60] implemented in the ROOT package TMVA [61]. These classifiers are trained on half of the signal and background events, and validated with the other half. Choice of the BDT input variables aims to achieve a robust signal-to-background discrimination ensuring low inter-variable correlation.

In the ggH category, simulated signal and data events from the meson mass sidebands defined in Section 4 are used as training and test samples. The BDT is based on four variables: the ratio of the meson p_T to the photon and ditrack three-body mass ($m_{M\gamma}$), $p_T^M/m_{M\gamma}$; the ratio of the photon p_T and $m_{M\gamma}$, $p_T^\gamma/m_{M\gamma}$; the meson pseudorapidity; and the isolation of the leading meson track candidate,

$$I^{ch}(\text{trk}_1) = \frac{p_T^{\text{trk}_1}}{p_T^{\text{trk}_1} + \sum_{ch} |p_T^{ch}|}, \tag{2}$$

where $\sum_{ch} |p_T^{ch}|$ is defined as in Eq. (1). Regarding the ratio variables, the photon and meson p_T are divided by $m_{M\gamma}$ in order to decrease their correlation with the Higgs boson mass estimate.

In the VBF categories, background from simulated photon plus jet events and photon plus ditrack data events are used for training and testing. In the data events, the two tracks are required to have the same charge. The list of BDT variables used is as follows: $p_T^M/m_{M\gamma}$; p_T^γ; $p_T^{M\gamma}$; the photon identification discriminator; the meson charged isolation; M_{jj}; the $\Delta\phi$ of the two tagging jets; and the Zeppenfeld variable, defined as $z^* = |\eta_{M\gamma} - 0.5(\eta_{j1} + \eta_{j2})|/|\Delta\eta_{jj}|$ [62].

Each event category employing a BDT-based classification is further split in two sub-categories of different purity, cat0 and cat1, where the BDT score thresholds of the two sub-categories have been optimized for a maximal value of $\varepsilon/\sqrt{B}$. Here ε and B denote the signal efficiency and number of expected events of the $m_{M\gamma}$ distribution, within a range of ±3 standard deviations centered around the Higgs boson mass, for the given BDT score selection. In each case, the two sub-categories are analyzed separately for signal extraction. Events with a BDT-score below the lowest threshold (cat1) are discarded. Table 2 summarizes selection criteria for all event categories.

7. Modeling of the H candidate mass distribution and analysis strategy

The $m_{M\gamma}$ distributions are used in the signal extraction. If multiple photon and ditrack candidates are selected in an event, only the one with

Table 2
Summary of the event selection criteria, photon identification efficiency and integrated luminosity ($\mathcal{L}$) used in the analysis.

	Common selections			
M selection	2 "high-purity" tracks, opposite charge $\|\eta^{\mathrm{trk}}\| < 2.5$, $p_{\mathrm{T}}^{\mathrm{trk1}} > 20\,\mathrm{GeV}$, $p_{\mathrm{T}}^{\mathrm{trk2}} > 5\,\mathrm{GeV}$, $\|\eta^{\mathrm{M}}\| < 2.1$ $0.62 < m_{\pi\pi} < 0.92\,\mathrm{GeV}$ (ρ^0)/$1.008 < m_{\mathrm{KK}} < 1.032\,\mathrm{GeV}$ (ϕ)/$0.84 < m_{\mathrm{K}\pi} < 0.94\,\mathrm{GeV}$ (K^{*0})			
Category	ggH	VBF High-p_{T}^{γ}	VBF Low-p_{T}^{γ}	VH
$\mathcal{L}$	$39.5\,\mathrm{fb}^{-1}$	$86.9\,\mathrm{fb}^{-1}$	$39.5\,\mathrm{fb}^{-1}$	$138\,\mathrm{fb}^{-1}$
Trigger	γ + jet with τ-ID	High-p_{T} γ + VBF-like jets	γ + jet with τ-ID	Double or single e/μ
p_{T}^{γ} (GeV)	>38	>75	>38 and <75	>40
$\|\eta^{\gamma}\|$	<2.5	<1.4	<2.1	<2.5
γ-ID (eff.)	80%	90%	80%	90%
$p_{\mathrm{T}}^{\mathrm{M}}$ (GeV)	>38	>30	>38	>40
I^{ch}(M)	>0.9	>0.9	>0.9	>0.8
I^{neu}(M)	>0.8	—	—	—
Event tagging	Meson candidate within a jet with $p_{\mathrm{T}}^{\mathrm{j}} > 40\,\mathrm{GeV}$, tracks with $\Delta R < 0.07$	2 jets with $p_{\mathrm{T}}^{\mathrm{j}} > 40\,\mathrm{GeV}$ $m_{\mathrm{jj}} > 400\,\mathrm{GeV}$ $\|\Delta\eta_{\mathrm{jj}}\| > 3$	2 jets with $p_{\mathrm{T}}^{\mathrm{j}} > 30/20\,\mathrm{GeV}$ $m_{\mathrm{jj}} > 300\,\mathrm{GeV}$ $\|\Delta\eta_{\mathrm{jj}}\| > 3$	1 selected and isolated e/μ or 2 selected e/μ $\|M_{\ell\ell} - M_{\mathrm{Z}}\| < 15\,\mathrm{GeV}$
Veto	e/μ, VBF-like jets	e/μ	e/μ	—
	BDT categories			
cat0	BDT > 0.55	BDT > 0.7	BDT > 0.7	—
cat1	−0.4 < BDT < 0.55	−0.6 < BDT < 0.7	−0.6 < BDT < 0.7	—

the largest p_{T} is retained to form the Higgs boson candidate. The analysis categories and the three data-taking periods, corresponding to the years 2016, 2017, and 2018, are considered as separate contributions in a simultaneous fit.

In each category and decay channel, the $m_{\mathrm{M}\gamma}$ signal distributions are described by analytical functions with their parameters determined through unbinned maximum likelihood fits to the respective samples. Based on the simulated signal events, the shape of the $m_{\mathrm{M}\gamma}$ distribution is approximated by a double-sided Crystal Ball function (DSCB) [63]. The values of the DSCB parameters, extracted from fits to simulated signals in different categories and decay channels, are fixed in the final fits to data.

The background parametrization is determined with fits in the $m_{\mathrm{M}\gamma}$ spectrum sidebands $m_L < m_{\mathrm{M}\gamma} < 120\,\mathrm{GeV}$ and $130\,\mathrm{GeV} < m_{\mathrm{M}\gamma} < m_R$, where $\{m_L, m_R\} = \{100, 150\}\,\mathrm{GeV}$ for the leptonic decay, $\{m_L, m_R\} = \{100, 170\}\,\mathrm{GeV}$ for the high-p_{T}^{γ} VBF category, and $\{m_L, m_R\} = \{110, 160\}\,\mathrm{GeV}$ for the remaining ones. We use Chebychev and Bernstein polynomials, along with exponential functions to model the background shape.

The optimal order of polynomial functions, that vary between two and four depending on the category and decay channel, is determined using a Fisher statistical test [64]. All parameters of the functions are allowed to float freely in the final fits to data. The potential bias due to the choice of the background parametrization is evaluated by generating pseudo-experiments following the distribution of one of the background models. Amounts of signal corresponding to branching fractions of 10^{-5} are also added to pseudo-data. Extended unbinned maximum likelihood fits, using an alternative background model, are performed to extract the branching fraction from each pseudo-experiment. The median difference between the measured and injected signal yields, relative to the post-fit uncertainty in the signal yields, gives an estimate of the bias induced by the choice of the fitting function as background model. The measured biases are found to be smaller than 20% across all background parametrizations. Including these observed deviations as spurious signals leads to a negligible change in the overall uncertainty of the measured signal rate of less than 1%. For the final systematic uncertainty estimation related to the background shape, including a possible bias, all tested background parametrizations are employed in a discrete profiling method [65] described in the following.

8. Systematic uncertainties

To estimate systematic uncertainties related to the choice of the $m_{\mathrm{M}\gamma}$ analytical background shapes, a discrete profiling method is used, which treats the choice of a specific model as a discrete nuisance parameter in the fit. Several systematic uncertainties affect the normalization of the simulated signal templates; they are included in the likelihood function as nuisance parameters and are profiled when minimizing it.

i. The uncertainties in the integrated luminosity measurements range between 1.2 and 2.5%, depending on data-taking period [66–68].
ii. The uncertainty in the total inelastic cross section, used for correcting the PU profile in simulation to the profile in data, is 4.6% [69]. The effect of this uncertainty on the signal normalization amounts to approximately 1%.
iii. Uncertainties in the efficiency of the photon plus τ-like jet trigger are 2.2–3.4% for the photon part and 5.3–5.6% for the ditrack part.
iv. Photon identification efficiencies are derived from $\mathrm{Z} \to \mathrm{ee}$ events and their uncertainty is propagated to the selection efficiency [28]. The uncertainties are p_{T} and η dependent and are at most 1.5%.
v. The uncertainty in the tracking efficiency amounts to 2.3–2.4% per track, corresponding to 4.6–4.8% per ditrack, depending on the data-taking period. This uncertainty is determined by comparing ratios of D^{*0} meson decay chains in data and simulation [70].
vi. Uncertainties in the muon and electron identification, isolation, and trigger efficiencies arise from the method used to obtain those efficiencies and from the limited size of the simulated samples used in these studies. They amount to less than 1.0% (1.5%) for muons (electrons) [27,28].
vii. Uncertainties affecting the charged and neutral meson isolation efficiencies are taken as the maximum difference between the efficiency as measured in data dimuon events and in simulated signal events. It ranges from 1.7% to 2.8%, depending on the decay channel and the type of isolation.
viii. Uncertainties in jet energy scale and resolution corrections are only relevant for the VBF categories and are smaller than 3.5%.
ix. The theoretical QCD scale uncertainty is calculated by varying the renormalization and factorization scales. The maximum and minimum envelope of the resulting distributions are taken as the up/down variations. These uncertainties amount to 3.9% for the

Table 3
Exclusion limits at 95% CL on the branching fractions of the Higgs boson decays. The limits are reported for the four categories (with subcategories combined, where applicable) and for their overall combination. Observed and median expected limits with the upper and lower bounds in the expected 68% CL intervals are also reported.

	$\mathcal{B}(\mathrm{H} \to \rho^0\gamma)$		$\mathcal{B}(\mathrm{H} \to \phi\gamma)$		$\mathcal{B}(\mathrm{H} \to \mathrm{K}^{*0}\gamma)$	
Category	Exp.($\times10^{-4}$)	Obs.($\times10^{-4}$)	Exp.($\times10^{-4}$)	Obs.($\times10^{-4}$)	Exp.($\times10^{-4}$)	Obs.($\times10^{-4}$)
VH	62^{+26}_{-18}	74	37^{+17}_{-11}	45	38^{+17}_{-11}	73
Low-p_{T}^{γ} VBF	50^{+23}_{-15}	36	33^{+19}_{-12}	28	29^{+13}_{-9}	19
High-p_{T}^{γ} VBF	23^{+11}_{-7}	16	16^{+9}_{-6}	11	14^{+7}_{-4}	10
ggH	$6.0^{+2.5}_{-1.7}$	4.4	$3.1^{+1.3}_{-1.0}$	3.5	$3.3^{+1.3}_{-1.0}$	3.4
Combined	$5.7^{+2.4}_{-1.6}$	3.7	$2.9^{+1.3}_{-0.8}$	3.0	$3.1^{+1.3}_{-0.9}$	3.0

ggH production cross section. For the VBF, WH, ZH, and $\mathrm{t\bar{t}H}$ production cross sections, the uncertainties are 0.4%, 0.7%, 3.8%, and 2.6%, respectively [39].

x. Uncertainties from the choice of PDF set and the value of the strong coupling constant (α_S) depend on the Higgs boson production mode and range from 1.6 to 3.2%. These uncertainties are derived through reweighting the events with several alternative sets of weights. These weights are derived according to the prescriptions in PDF4LHC [71] and NNPDF3.1 [43].

xi. Parton shower modeling uncertainties arise from the renormalization scale of QCD-induced initial-state radiation (ISR) and FSR in PYTHIA. Variations of renormalization parameters of the ISR and FSR consist of four combinations obtained by keeping one constant and doubling or halving the other. The corresponding uncertainties are in the range 1.0–3.0%.

The largest impact on the UL is from the background shape uncertainties. Uncertainties in the signal yield from the acceptance effects in theory calculations are found to be negligible, as are those arising from the photon energy scale and resolution.

Theoretical uncertainties in the production cross sections, and the uncertainties due to the choice of PDF set and the value of α_S are treated as correlated between the different data-taking periods. The uncertainty in the integrated luminosity measurement is treated as partially correlated between these periods. The other experimental uncertainties are treated as uncorrelated between the different data-taking periods.

9. Results

The results of this analysis have been determined using the CMS statistical analysis tool COMBINE [72]. The $m_{\mathrm{M}\gamma}$ distributions in data and the background estimations are shown in Fig. 3 for some selected analysis categories. The $\mathrm{H} \to \rho^0\gamma$, $\mathrm{H} \to \phi\gamma$, and $\mathrm{H} \to \mathrm{K}^{*0}\gamma$ signals are also shown, normalized to the UL of the branching fractions expected for the selected categories. No excess above the background expectation is observed. The results are presented as UL on $\mathcal{B}(\mathrm{H} \to \rho^0\gamma)$, $\mathcal{B}(\mathrm{H} \to \phi\gamma)$, and $\mathcal{B}(\mathrm{H} \to \mathrm{K}^{*0}\gamma)$ set at 95% confidence level (CL). Limits are set using the modified frequentist $\mathrm{CL_s}$ approach [73,74], in which a profile-likelihood ratio modified for UL setting is used as the test statistic, making use of the asymptotic approximation [75]. Systematic uncertainties are incorporated in the likelihood as nuisance parameters. Fig. 4 reports the expected and observed 95% CL UL according to analysis category, where the two BDT-based sub-categories of ggH and VBF have been merged. The ggH category dominates the search sensitivity for all decay channels. By combining all the categories, the observed (expected) UL on $\mathcal{B}(\mathrm{H} \to \rho^0\gamma)$, $\mathcal{B}(\mathrm{H} \to \phi\gamma)$, and $\mathcal{B}(\mathrm{H} \to \mathrm{K}^{*0}\gamma)$ are 3.7×10^{-4} (5.7×10^{-4}), 3.0×10^{-4} (2.9×10^{-4}), and 3.0×10^{-4} (3.1×10^{-4}), respectively. These values correspond to 22 times the SM expectation for the $\mathrm{H} \to \rho^0\gamma$ decay and 129 times the SM expectation for the $\mathrm{H} \to \phi\gamma$ decay. For the strongly suppressed $\mathrm{H} \to \mathrm{K}^{*0}\gamma$ decay, this limit corresponds to 3.0×10^{15} times the value expected in the SM. The observed and median expected exclusion limits for the branching fractions at 95% CL for the Higgs boson decays are listed in Table 3.

10. Summary

A search was presented for Higgs boson decays into a photon and a $\rho(770)^0$, $\phi(1020)$, or $\mathrm{K}^*(892)^0$ meson, using pp collision data at $\sqrt{s} = 13\,\mathrm{TeV}$ collected by the CMS experiment at the LHC. Events are selected assuming the mesons decay into a pair of charged pions, a pair of charged kaons, or a charged kaon and pion, respectively. Depending on the Higgs boson production mode, different signal triggering and reconstruction techniques are adopted. The analyzed data sets correspond to an integrated luminosity varying between 39.5 and $138\,\mathrm{fb}^{-1}$, depending on the targeted final state. After combining various data sets and categories, no significant excess above the background expectations is observed. Upper limits at the 95% confidence level on the Higgs boson branching fractions into $\rho(770)^0\gamma$, $\phi(1020)\gamma$, and $\mathrm{K}^*(892)^0\gamma$ are determined to be 3.7×10^{-4}, 3.0×10^{-4}, and 3.0×10^{-4}, respectively. Limits for the $\rho(770)^0\gamma$ and $\phi(1020)\gamma$ channels constitute the most stringent experimental limits to date.

Declaration of competing interest

The authors declare that they have no known competing financial interests or personal relationships that could have appeared to influence the work reported in this paper.

Acknowledgements

We congratulate our colleagues in the CERN accelerator departments for the excellent performance of the LHC and thank the technical and administrative staffs at CERN and at other CMS institutes for their contributions to the success of the CMS effort. In addition, we gratefully acknowledge the computing centres and personnel of the Worldwide LHC Computing Grid and other centres for delivering so effectively the computing infrastructure essential to our analyses. Finally, we acknowledge the enduring support for the construction and operation of the LHC, the CMS detector, and the supporting computing infrastructure provided by the following funding agencies: SC (Armenia), BMBWF and FWF (Austria); FNRS and FWO (Belgium); CNPq, CAPES, FAPERJ, FAPERGS, and FAPESP (Brazil); MES and BNSF (Bulgaria); CERN; CAS, MOST, and NSFC (China); Minciencias (Colombia); MSES and CSF (Croatia); RIF (Cyprus); SENESCYT (Ecuador); ERC PRG, RVTT3 and MoER TK202 (Estonia); Academy of Finland, MEC, and HIP (Finland); CEA and CNRS/IN2P3 (France); SRNSF (Georgia); BMBF, DFG, and HGF (Germany); GSRI (Greece); NKFIH (Hungary); DAE and DST (India); IPM (Iran); SFI (Ireland); INFN (Italy); MSIP and NRF (Republic of Korea); MES (Latvia); LMTLT (Lithuania); MOE and UM (Malaysia); BUAP, CINVESTAV, CONACYT, LNS, SEP, and UASLP-FAI (Mexico); MOS (Montenegro); MBIE (New Zealand); PAEC (Pakistan); MES and NSC (Poland); FCT (Portugal); MESTD (Serbia); MCIN/AEI and PCTI (Spain); MoSTR (Sri Lanka); Swiss Funding Agencies (Switzerland); MST (Taipei); MHESI and NSTDA (Thailand); TUBITAK and TENMAK (Turkey); NASU (Ukraine); STFC (United Kingdom); DOE and NSF (USA).

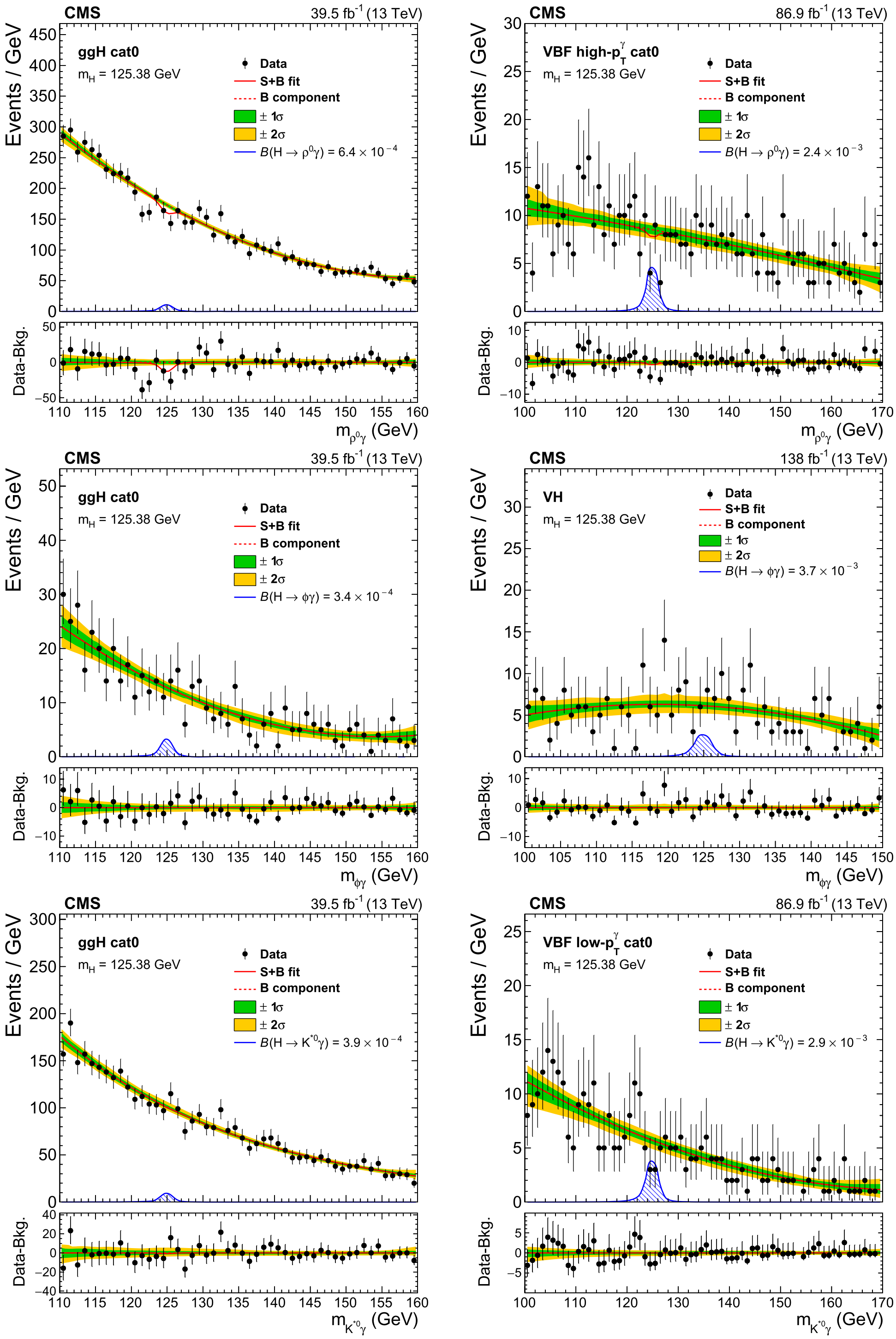

Fig. 3. Post-fit $m_{\mathrm{M}\gamma}$ distributions in data and the background model for ggH cat0 (upper left) and VBF high-p_{T}^{γ} cat0 (upper right) of the $\mathrm{H} \to \rho^0\gamma$ search, ggH cat0 (middle left) and the VH category (middle right) of the $\mathrm{H} \to \phi\gamma$ search, ggH cat0 (lower left) and the VBF low-p_{T}^{γ} cat0 (lower right) of the $\mathrm{H} \to \mathrm{K}^{*0}\gamma$ search. The signal simulation is shown normalized at a branching fraction corresponding to the expected UL. Signal and background fit components, as well as 1 and 2 standard deviation(s) uncertainty bands are also shown.

Individuals have received support from the Marie-Curie programme and the European Research Council and Horizon 2020 Grant, contract Nos. 675440, 724704, 752730, 758316, 765710, 824093, 101115353, 101002207, and COST Action CA16108 (European Union); the Leventis Foundation; the Alfred P. Sloan Foundation; the Alexander von Humboldt Foundation; the Science Committee, project no. 22rl-037 (Armenia); the Belgian Federal Science Policy Office; the Fonds pour la Formation à la Recherche dans l'Industrie et dans l'Agriculture (FRIA-Belgium); the F.R.S.-FNRS and FWO (Belgium) under the "Excellence of Science – EOS" – be.h project n. 30820817; the Beijing Municipal Science & Technology Commission, No. Z191100007219010 and Fundamental Research Funds for the Central Universities (China); The Ministry of Education, Youth and Sports (MEYS) of the Czech Republic; the Shota Rustaveli National Science Foundation, grant FR-22-985 (Georgia); the Deutsche Forschungsgemeinschaft (DFG), among others, under Germany's Excellence Strategy – EXC 2121 "Quantum Uni-

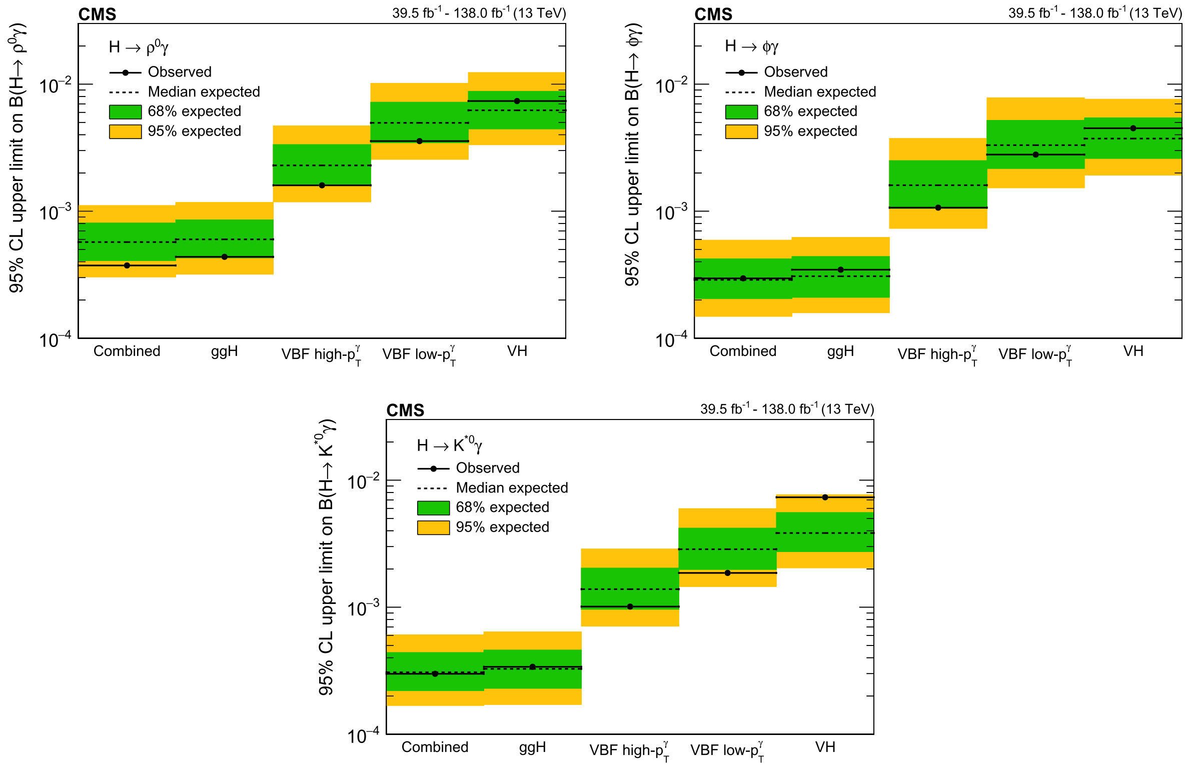

Fig. 4. Expected and observed UL on $\mathcal{B}(\mathrm{H} \to \rho^0\gamma)$ (upper left), $\mathcal{B}(\mathrm{H} \to \phi\gamma)$ (upper right), and $\mathcal{B}(\mathrm{H} \to \mathrm{K}^{*0}\gamma)$ (lower) split by analysis categories (with subcategories combined, where applicable) and their overall combination. Green and yellow bands correspond to 68% and 95% confidence intervals on the expected upper limits.

verse" – 390833306, and under project number 400140256 - GRK2497; the Hellenic Foundation for Research and Innovation (HFRI), Project Number 2288 (Greece); the Hungarian Academy of Sciences, the New National Excellence Program - ÚNKP, the NKFIH research grants K 131991, K 133046, K 138136, K 143460, K 143477, K 146913, K 146914, K 147048, 2020-2.2.1-ED-2021-00181, and TKP2021-NKTA-64 (Hungary); the Council of Science and Industrial Research, India; ICSC – National Research Centre for High Performance Computing, Big Data and Quantum Computing and FAIR – Future Artificial Intelligence Research, funded by the NextGenerationEU program (Italy); the Latvian Council of Science; the Ministry of Education and Science, project no. 2022/WK/14, and the National Science Center, contracts Opus 2021/41/B/ST2/01369 and 2021/43/B/ST2/01552 (Poland); the Fundação para a Ciência e a Tecnologia, grant CEECIND/01334/2018 (Portugal); the National Priorities Research Program by Qatar National Research Fund; the Ministry of Science and Higher Education, projects no. FSWU-2023-0073 and no. FSWW-2020-0008 (Russia); MCIN/AEI/10.13039/501100011033, ERDF "a way of making Europe", and the Programa Estatal de Fomento de la Investigación Científica y Técnica de Excelencia María de Maeztu, grant MDM-2017-0765 and Programa Severo Ochoa del Principado de Asturias (Spain); the Chulalongkorn Academic into Its 2nd Century Project Advancement Project, and the National Science, Research and Innovation Fund via the Program Management Unit for Human Resources & Institutional Development, Research and Innovation, grant B39G670016 (Thailand); the Kavli Foundation; the Nvidia Corporation; the SuperMicro Corporation; the Welch Foundation, contract C-1845; and the Weston Havens Foundation (USA).

Data availability

Release and preservation of data used by the CMS Collaboration as the basis for publications is guided by the CMS data preservation, re-use and open access policy.

References

[1] ATLAS Collaboration, Observation of a new particle in the search for the standard model Higgs boson with the ATLAS detector at the LHC, Phys. Lett. B 716 (2012) 1, https://doi.org/10.1016/j.physletb.2012.08.020, arXiv:1207.7214.

[2] CMS Collaboration, Observation of a new boson at a mass of 125 GeV with the CMS experiment at the LHC, Phys. Lett. B 716 (2012) 30, https://doi.org/10.1016/j.physletb.2012.08.021, arXiv:1207.7235.

[3] CMS Collaboration, Observation of a new boson with mass near 125 GeV in pp collisions at $\sqrt{s}$ = 7 and 8 TeV, J. High Energy Phys. 06 (2013) 081, https://doi.org/10.1007/JHEP06(2013)081, arXiv:1303.4571.

[4] ATLAS Collaboration, Observation of Higgs boson production in association with a top quark pair at the LHC with the ATLAS detector, Phys. Lett. B 784 (2018) 173, https://doi.org/10.1016/j.physletb.2018.07.035, arXiv:1806.00425.

[5] CMS Collaboration, Observation of $\mathrm{t\bar{t}H}$ production, Phys. Rev. Lett. 120 (2018) 231801, https://doi.org/10.1103/PhysRevLett.120.231801, arXiv:1804.02610.

[6] ATLAS Collaboration, Measurements of Higgs boson production cross-sections in the $H \to \tau^+\tau^-$ decay channel in pp collisions at $\sqrt{s}$ = 13 TeV with the ATLAS detector, J. High Energy Phys. 08 (2022) 175, https://doi.org/10.1007/JHEP08(2022)175, arXiv:2201.08269.

[7] CMS Collaboration, Measurement of the inclusive and differential Higgs boson production cross sections in the decay mode to a pair of τ leptons in pp collisions at $\sqrt{s}$ = 13 TeV, Phys. Rev. Lett. 128 (2022), https://doi.org/10.1103/PhysRevLett.128.081805, arXiv:2107.11486.

[8] CMS Collaboration, Measurements of Higgs boson production in the decay channel with a pair of τ leptons in proton-proton collisions at $\sqrt{s}$ = 13 TeV, Eur. Phys. J. C 83 (2023) 562, https://doi.org/10.1140/epjc/s10052-023-11452-8, arXiv:2204.12957.

[9] ATLAS Collaboration, Measurements of WH and ZH production in the $H \to b\bar{b}$ decay channel in pp collisions at 13 TeV with the ATLAS detector, Eur. Phys. J. C 81 (2021) 178, https://doi.org/10.1140/epjc/s10052-020-08677-2, arXiv:2007.02873.

[10] CMS Collaboration, Observation of the Higgs boson decay to bottom quarks, Phys. Rev. Lett. 121 (2018) 121801, https://doi.org/10.1103/PhysRevLett.121.121801, arXiv:1808.08242.

[11] ATLAS Collaboration, Direct constraint on the Higgs-charm coupling from a search for Higgs boson decays into charm quarks with the ATLAS detector, Eur. Phys. J. C 82 (2022) 717, https://doi.org/10.1140/epjc/s10052-022-10588-3, arXiv:2201.11428.

[12] CMS Collaboration, Search for Higgs boson decay to a charm quark-antiquark pair in proton-proton collisions at $\sqrt{s}$ = 13 TeV, Phys. Rev. Lett. 131 (2023), https://doi.org/10.1103/PhysRevLett.131.061801, arXiv:2205.05550.

[13] CMS Collaboration, Search for Higgs boson decays into Z and J/ψ and for Higgs and Z boson decays into J/ψ or Υ pairs in pp collisions at $\sqrt{s}$ = 13 TeV, Phys. Lett. B (2023), https://doi.org/10.1016/j.physletb.2022.137534, arXiv:2206.03525.

[14] ATLAS Collaboration, Searches for exclusive Higgs and Z boson decays into a vector quarkonium state and a photon using 139 fb^{-1} of ATLAS $\sqrt{s} = 13$ TeV proton-proton collision data, Eur. Phys. J. C 83 (2023), https://doi.org/10.1140/epjc/s10052-023-11869-1, arXiv:2208.03122.

[15] CMS Collaboration, Search for rare decays of Z and Higgs bosons to J/ψ and a photon in proton-proton collisions at $\sqrt{s} = 13$ TeV, Eur. Phys. J. C 79 (2019), https://doi.org/10.1140/epjc/s10052-019-6562-5, arXiv:1810.10056.

[16] CMS Collaboration, Evidence for Higgs boson decay to a pair of muons, J. High Energy Phys. 01 (2021) 148, https://doi.org/10.1007/JHEP01(2021)148, arXiv:2009.04363.

[17] A.L. Kagan, G. Perez, F. Petriello, Y. Soreq, S. Stoynev, J. Zupan, Exclusive window onto Higgs Yukawa couplings, Phys. Rev. Lett. 114 (2015), https://doi.org/10.1103/PhysRevLett.114.101802, arXiv:1406.1722.

[18] CMS Collaboration, Search for decays of the 125 GeV Higgs boson into a Z boson and a ρ or ϕ meson, J. High Energy Phys. 11 (2020) 039, https://doi.org/10.1007/JHEP11(2020)039, arXiv:2007.05122.

[19] ATLAS Collaboration, Search for exclusive Higgs and z boson decays to $\phi\gamma$ and $\rho\gamma$ with the ATLAS detector, J. High Energy Phys. 12 (2023) 127, https://doi.org/10.1007/JHEP12(2023)158, arXiv:1712.02758.

[20] ATLAS Collaboration, Search for exclusive Higgs and Z boson decays to $\omega\gamma$ and Higgs boson decays to $K^*\gamma$ with the ATLAS detector, Phys. Lett. B 847 (2023), https://doi.org/10.1016/j.physletb.2023.138292, arXiv:2301.09938.

[21] ATLAS Collaboration, Searches for exclusive Higgs boson decays into $D^*\gamma$ and Z boson decays into $D^0\gamma$ and $K_s^0\gamma$ in pp collisions at $\sqrt{s} = 13$ TeV with the ATLAS detector, Phys. Lett. B 847 (2024), https://doi.org/10.48550/arXiv.2402.18731, arXiv:2402.18731.

[22] M. König, M. Neubert, Exclusive radiative Higgs decays as probes of light-quark Yukawa couplings, J. High Energy Phys. 08 (2015) 012, https://doi.org/10.1007/JHEP08(2015)012, arXiv:1505.03870.

[23] G. Perez, Y. Soreq, E. Stamou, K. Tobioka, Prospects for measuring the Higgs boson coupling to light quarks, Phys. Rev. D 93 (2016) 013001, https://doi.org/10.1103/PhysRevD.93.013001, arXiv:1505.06689.

[24] D. d'Enterria, V.D. Le, Rare and exclusive few-body decays of the Higgs, Z, W bosons, and the top quark, J. Phys. G (2024), https://doi.org/10.1088/1361-6471/ad3c59, arXiv:2312.11211.

[25] HEPData record for this analysis, https://doi.org/10.17182/hepdata.154745, 2024.

[26] CMS Collaboration, Description and performance of track and primary-vertex reconstruction with the CMS tracker, J. Instrum. 9 (2014) P10009, https://doi.org/10.1088/1748-0221/9/10/P10009, arXiv:1405.6569.

[27] CMS Collaboration, Performance of the CMS muon detector and muon reconstruction with proton-proton collisions at $\sqrt{s} = 13$ TeV, J. Instrum. 13 (2018) P06015, https://doi.org/10.1088/1748-0221/13/06/P06015, arXiv:1804.04528.

[28] CMS Collaboration, Electron and photon reconstruction and identification with the CMS experiment at the CERN LHC, J. Instrum. 16 (2021), https://doi.org/10.1088/1748-0221/16/05/P05014, arXiv:2012.06888.

[29] CMS Collaboration, The CMS trigger system, J. Instrum. 12 (2017) P01020, https://doi.org/10.1088/1748-0221/12/01/P01020, arXiv:1609.02366.

[30] CMS Collaboration, Performance of the CMS level-1 trigger in proton-proton collisions at $\sqrt{s} = 13$ TeV, J. Instrum. 15 (2020) P10017, https://doi.org/10.1088/1748-0221/15/10/P10017, arXiv:2006.10165.

[31] CMS Collaboration, Performance of the CMS high-level trigger during LHC run 2, J. Instrum. 19 (2024) P11021, https://doi.org/10.1088/1748-0221/19/11/P11021, arXiv:2410.17038.

[32] CMS Collaboration, The CMS experiment at the CERN LHC, J. Instrum. 3 (2008) S08004, https://doi.org/10.1088/1748-0221/3/08/S08004.

[33] P. Nason, A new method for combining NLO QCD with shower Monte Carlo algorithms, J. High Energy Phys. 11 (2004) 040, https://doi.org/10.1088/1126-6708/2004/11/040, arXiv:hep-ph/0409146.

[34] S. Frixione, P. Nason, C. Oleari, Matching NLO QCD computations with parton shower simulations: the POWHEG method, J. High Energy Phys. 11 (2007) 070, https://doi.org/10.1088/1126-6708/2007/11/070, arXiv:0709.2092.

[35] S. Alioli, P. Nason, C. Oleari, E. Re, NLO Higgs boson production via gluon fusion matched with shower in POWHEG, J. High Energy Phys. 04 (2009) 002, https://doi.org/10.1088/1126-6708/2009/04/002, arXiv:0812.0578.

[36] S. Alioli, P. Nason, C. Oleari, E. Re, A general framework for implementing NLO calculations in shower Monte Carlo programs: the POWHEG BOX, J. High Energy Phys. 06 (2010) 043, https://doi.org/10.1007/JHEP06(2010)043, arXiv:1002.2581.

[37] P. Nason, C. Oleari, NLO Higgs boson production via vector-boson fusion matched with shower in POWHEG, J. High Energy Phys. 02 (2010) 037, https://doi.org/10.1007/JHEP02(2010)037, arXiv:0911.5299.

[38] G. Luisoni, P. Nason, C. Oleari, F. Tramontano, HW$^{\pm}$/HZ + 0 and 1 jet at NLO with the POWHEG BOX interfaced to GoSam and their merging within MiNLO, J. High Energy Phys. 10 (2013) 083, https://doi.org/10.1007/JHEP10(2013)083, arXiv:1306.2542.

[39] L.H.C. Higgs, Cross section working group, handbook of LHC Higgs cross sections: 4. Deciphering the nature of the Higgs sector, CERN Yellow Rep. Monogr. (2016), https://doi.org/10.23731/CYRM-2017-002, arXiv:1610.07922.

[40] Particle Data Group, S. Navas, et al., Review of particle physics, Phys. Rev. D 110 (2024) 030001, https://doi.org/10.1103/PhysRevD.110.030001.

[41] J. Alwall, R. Frederix, S. Frixione, V. Hirschi, F. Maltoni, O. Mattelaer, H.S. Shao, T. Stelzer, P. Torrielli, M. Zaro, The automated computation of tree-level and next-to-leading order differential cross sections, and their matching to parton shower simulations, J. High Energy Phys. 07 (2014) 079, https://doi.org/10.1007/JHEP07(2014)079, arXiv:1405.0301.

[42] R. Frederix, S. Frixione, Merging meets matching in MC@NLO, J. High Energy Phys. 12 (2012) 061, https://doi.org/10.1007/JHEP12(2012)061, arXiv:1209.6215.

[43] R.D. Ball, et al., NNPDF, Parton distributions from high-precision collider data, Eur. Phys. J. C 77 (2017) 663, https://doi.org/10.1140/epjc/s10052-017-5199-5, arXiv:1706.00428.

[44] T. Sjöstrand, S. Ask, J.R. Christiansen, R. Corke, N. Desai, P. Ilten, S. Mrenna, S. Prestel, C.O. Rasmussen, P.Z. Skands, An introduction to PYTHIA 8.2, Comput. Phys. Commun. 191 (2015) 159, https://doi.org/10.1016/j.cpc.2015.01.024, arXiv:1410.3012.

[45] CMS Collaboration, Extraction and validation of a new set of CMS PYTHIA8 tunes from underlying-event measurements, Eur. Phys. J. C 80 (2020) 4, https://doi.org/10.1140/epjc/s10052-019-7499-4, arXiv:1903.12179.

[46] P. Faccioli, C. Lourenço, Particle Polarization in High Energy Physics; an Introduction and Case Studies on Vector Particle Production at the LHC, Lecture Notes in Physics, vol. 1002, Springer, 2022.

[47] D.J. Lange, The EvtGen particle decay simulation package, Nucl. Instrum. Methods A 462 (2001) 152, https://doi.org/10.1016/S0168-9002(01)00089-4.

[48] S. Agostinelli, et al., Geant4, Geant4—a simulation toolkit, Nucl. Instrum. Methods A 506 (2003) 250, https://doi.org/10.1016/S0168-9002(03)01368-8.

[49] CMS Collaboration, Particle-flow reconstruction and global event description with the CMS detector, J. Instrum. 12 (2017) P10003, https://doi.org/10.1088/1748-0221/12/10/P10003, arXiv:1706.04965.

[50] D. Contardo, M. Klute, J. Mans, L. Silvestris, J. Butler, Technical Proposal for the Phase-II Upgrade of the CMS Detector, Technical Report CMS-TDR-15-02, CERN, Geneva, 2015.

[51] CMS Collaboration, Measurements of inclusive W and Z cross sections in pp collisions at $\sqrt{s} = 7$ TeV, J. High Energy Phys. 01 (2011) 080, https://doi.org/10.1007/JHEP01(2011)080, arXiv:1012.2466.

[52] M. Cacciari, G.P. Salam, G. Soyez, The catchment area of jets, J. High Energy Phys. 04 (2008) 005, https://doi.org/10.1088/1126-6708/2008/04/005, arXiv:0802.1188.

[53] M. Cacciari, G.P. Salam, G. Soyez, The anti-k_T jet clustering algorithm, J. High Energy Phys. 04 (2008) 063, https://doi.org/10.1088/1126-6708/2008/04/063, arXiv:0802.1189.

[54] M. Cacciari, G.P. Salam, G. Soyez, FastJet user manual, Eur. Phys. J. C 72 (2012) 1896, https://doi.org/10.1140/epjc/s10052-012-1896-2, arXiv:1111.6097.

[55] CMS Collaboration, Pileup mitigation at CMS in 13 TeV data, J. Instrum. 15 (2020) P09018, https://doi.org/10.1088/1748-0221/15/09/P09018, arXiv:2003.00503.

[56] CMS Collaboration, Jet energy scale and resolution in the CMS experiment in pp collisions at 8 TeV, J. Instrum. 12 (2017), https://doi.org/10.1088/1748-0221/12/02/P02014, arXiv:1607.03663.

[57] E. Chabanat, J. D'Hondt, N. Estre, R. Fruhwirth, K. Prokofiev, T. Speer, P. Vanlaer, W. Waltenberger, Vertex reconstruction in CMS, Nucl. Instrum. Methods A 549 (2005) 188, https://doi.org/10.1016/j.nima.2005.04.050.

[58] CMS Collaboration, Performance of reconstruction and identification of τ leptons decaying to hadrons and ν_τ in pp collisions at $\sqrt{s} = 13$ TeV, J. Instrum. 13 (2018), https://doi.org/10.1088/1748-0221/13/10/P10005, arXiv:1809.02816.

[59] CMS Collaboration, Jet performance in pp collisions at $\sqrt{s} = 7$ TeV, CMS Physics Analysis Summary CMS-PAS-JME-10-003, https://cds.cern.ch/record/1279362/, 2010.

[60] T. Chen, C. Guestrin, XGBoost: a scalable tree boosting system, in: Proceedings of the 22nd ACM SIGKDD International Conference on Knowledge Discovery and Data Mining, KDD '16, ACM, New York, NY, USA, 2016, p. 785, arXiv:1603.02754.

[61] A. Hocker, et al., TMVA, TMVA - toolkit for multivariate data analysis, arXiv:physics/0703039, 2007.

[62] D.L. Rainwater, R. Szalapski, D. Zeppenfeld, Probing color singlet exchange in Z + 2-jet events at the CERN LHC, Phys. Rev. D 54 (1996) 6680, https://doi.org/10.1103/PhysRevD.54.6680, arXiv:hep-ph/9605444.

[63] M.J. Oreglia, A study of the reactions $\psi' \to \gamma\gamma\psi$, Ph.D. thesis, Stanford University, 1980, http://www.slac.stanford.edu/cgi-wrap/getdoc/slac-r-236.pdf, SLAC Report SLAC-R-236.

[64] R.D. Fisher, On the interpretation of χ^2 from contingency tables, and the calculation of P, J. R. Stat. Soc. 85 (1922) 87, https://doi.org/10.2307/2340521.

[65] P.D. Dauncey, M. Kenzie, N. Wardle, G.J. Davies, Handling uncertainties in background shapes: the discrete profiling method, J. Instrum. 10 (2015) P04015, https://doi.org/10.1088/1748-0221/10/04/P04015, arXiv:1408.6865.

[66] CMS Collaboration, Precision luminosity measurement in proton-proton collisions at $\sqrt{s} = 13$ TeV in 2015 and 2016 at CMS, Eur. Phys. J. C 81 (2021) 800, https://doi.org/10.1140/epjc/s10052-021-09538-2, arXiv:2104.01927.

[67] CMS Collaboration, CMS luminosity measurement for the 2017 data-taking period at $\sqrt{s} = 13$ TeV, CMS Physics Analysis Summary CMS-PAS-LUM-17-004, CERN, 2018, https://cds.cern.ch/record/2621960.

[68] CMS Collaboration, CMS luminosity measurement for the 2018 data-taking period at $\sqrt{s} = 13$ TeV, CMS Physics Analysis Summary CMS-PAS-LUM-18-002, CERN, 2019 https://cds.cern.ch/record/2676164.

[69] CMS Collaboration, Measurement of the inelastic proton-proton cross section at $\sqrt{s} = 13$ TeV, J. High Energy Phys. 07 (2018) 161, https://doi.org/10.1007/JHEP07(2018)161, arXiv:1802.02613.
[70] CMS Collaboration, Tracking performances for charged pions with Run2 Legacy data, Technical Report CMS-DP-2022-012, CERN, 2022, https://cds.cern.ch/record/2810814.
[71] J. Butterworth, et al., PDF4LHC recommendations for LHC run II, J. Phys. G 43 (2016) 023001, https://doi.org/10.1088/0954-3899/43/2/023001, arXiv:1510.03865.
[72] CMS Collaboration, The CMS statistical analysis and combination tool: combine, Comput. Softw. Big Sci. 8 (2024) 19, https://doi.org/10.1007/s41781-024-00121-4, arXiv:2404.06614.
[73] T. Junk, Confidence level computation for combining searches with small statistics, Nucl. Instrum. Methods A 434 (1999) 435, https://doi.org/10.1016/S0168-9002(99)00498-2, arXiv:hep-ex/9902006.
[74] A.L. Read, Presentation of search results: the CL_s technique, J. Phys. G 28 (2002) 2693, https://doi.org/10.1088/0954-3899/28/10/313.
[75] G. Cowan, K. Cranmer, E. Gross, O. Vitells, Asymptotic formulae for likelihood-based tests of new physics, Eur. Phys. J. C 71 (2011) 1554, https://doi.org/10.1140/epjc/s10052-011-1554-0, arXiv:1007.1727.

The CMS collaboration

A. Hayrapetyan, A. Tumasyan[1]

Yerevan Physics Institute, Yerevan, Armenia

W. Adam, J.W. Andrejkovic, T. Bergauer, S. Chatterjee, K. Damanakis, M. Dragicevic, P.S. Hussain, M. Jeitler[2], N. Krammer, A. Li, D. Liko, I. Mikulec, J. Schieck[2], R. Schöfbeck, D. Schwarz, M. Sonawane, W. Waltenberger, C.-E. Wulz[2]

Institut für Hochenergiephysik, Vienna, Austria

T. Janssen, T. Van Laer, P. Van Mechelen

Universiteit Antwerpen, Antwerpen, Belgium

N. Breugelmans, J. D'Hondt, S. Dansana, A. De Moor, M. Delcourt, F. Heyen, S. Lowette, I. Makarenko, D. Müller, S. Tavernier, M. Tytgat[3], G.P. Van Onsem, S. Van Putte, D. Vannerom

Vrije Universiteit Brussel, Brussel, Belgium

B. Bilin, B. Clerbaux, A.K. Das, G. De Lentdecker, H. Evard, L. Favart, P. Gianneios, J. Jaramillo, A. Khalilzadeh, F.A. Khan, K. Lee, M. Mahdavikhorrami, A. Malara, S. Paredes, M.A. Shahzad, L. Thomas, M. Vanden Bemden, C. Vander Velde, P. Vanlaer

Université Libre de Bruxelles, Bruxelles, Belgium

M. De Coen, D. Dobur, G. Gokbulut, Y. Hong, J. Knolle, L. Lambrecht, D. Marckx, K. Mota Amarilo, K. Skovpen, N. Van Den Bossche, J. van der Linden, L. Wezenbeek

Ghent University, Ghent, Belgium

A. Benecke, A. Bethani, G. Bruno, C. Caputo, J. De Favereau De Jeneret, C. Delaere, I.S. Donertas, A. Giammanco, A.O. Guzel, Sa. Jain, V. Lemaitre, J. Lidrych, P. Mastrapasqua, T.T. Tran, S. Wertz

Université Catholique de Louvain, Louvain-la-Neuve, Belgium

G.A. Alves, M. Alves Gallo Pereira, E. Coelho, G. Correia Silva, C. Hensel, T. Menezes De Oliveira, C. Mora Herrera[4], A. Moraes, P. Rebello Teles, M. Soeiro, A. Vilela Pereira[4]

Centro Brasileiro de Pesquisas Fisicas, Rio de Janeiro, Brazil

W.L. Aldá Júnior, M. Barroso Ferreira Filho, H. Brandao Malbouisson, W. Carvalho, J. Chinellato[5], E.M. Da Costa, G.G. Da Silveira[6], D. De Jesus Damiao, S. Fonseca De Souza, R. Gomes De Souza, T. Laux Kuhn, M. Macedo, J. Martins[7], L. Mundim, H. Nogima, J.P. Pinheiro, A. Santoro, A. Sznajder, M. Thiel

Universidade do Estado do Rio de Janeiro, Rio de Janeiro, Brazil

C.A. Bernardes [6], L. Calligaris, T.R. Fernandez Perez Tomei, E.M. Gregores, I. Maietto Silverio, P.G. Mercadante, S.F. Novaes, B. Orzari, Sandra S. Padula

Universidade Estadual Paulista, Universidade Federal do ABC, São Paulo, Brazil

A. Aleksandrov, G. Antchev, R. Hadjiiska, P. Iaydjiev, M. Misheva, M. Shopova, G. Sultanov

Institute for Nuclear Research and Nuclear Energy, Bulgarian Academy of Sciences, Sofia, Bulgaria

A. Dimitrov, L. Litov, B. Pavlov, P. Petkov, A. Petrov, E. Shumka

University of Sofia, Sofia, Bulgaria

S. Keshri, D. Laroze, S. Thakur

Instituto De Alta Investigación, Universidad de Tarapacá, Casilla 7 D, Arica, Chile

T. Cheng, T. Javaid, L. Yuan

Beihang University, Beijing, China

Z. Hu, Z. Liang, J. Liu

Department of Physics, Tsinghua University, Beijing, China

G.M. Chen [8], H.S. Chen [8], M. Chen [8], F. Iemmi, C.H. Jiang, A. Kapoor [9], H. Liao, Z.-A. Liu [10], R. Sharma [11], J.N. Song [10], J. Tao, C. Wang [8], J. Wang, Z. Wang [8], H. Zhang, J. Zhao

Institute of High Energy Physics, Beijing, China

A. Agapitos, Y. Ban, S. Deng, B. Guo, C. Jiang, A. Levin, C. Li, Q. Li, Y. Mao, S. Qian, S.J. Qian, X. Qin, X. Sun, D. Wang, H. Yang, L. Zhang, Y. Zhao, C. Zhou

State Key Laboratory of Nuclear Physics and Technology, Peking University, Beijing, China

S. Yang

Guangdong Provincial Key Laboratory of Nuclear Science and Guangdong-Hong Kong Joint Laboratory of Quantum Matter, South China Normal University, Guangzhou, China

Z. You

Sun Yat-Sen University, Guangzhou, China

K. Jaffel, N. Lu

University of Science and Technology of China, Hefei, China

G. Bauer [12], B. Li, K. Yi [13], J. Zhang

Nanjing Normal University, Nanjing, China

X. Gao [14], Y. Li

Institute of Modern Physics and Key Laboratory of Nuclear Physics and Ion-beam Application (MOE) - Fudan University, Shanghai, China

Z. Lin, C. Lu, M. Xiao

Zhejiang University, Hangzhou, Zhejiang, China

C. Avila, D.A. Barbosa Trujillo, A. Cabrera, C. Florez, J. Fraga, J.A. Reyes Vega

Universidad de Los Andes, Bogota, Colombia

F. Ramirez, C. Rendón, M. Rodriguez, A.A. Ruales Barbosa, J.D. Ruiz Alvarez

Universidad de Antioquia, Medellin, Colombia

D. Giljanovic, N. Godinovic, D. Lelas, A. Sculac

University of Split, Faculty of Electrical Engineering, Mechanical Engineering and Naval Architecture, Split, Croatia

M. Kovac, A. Petkovic, T. Sculac

University of Split, Faculty of Science, Split, Croatia

P. Bargassa, V. Brigljevic, B.K. Chitroda, D. Ferencek, K. Jakovcic, A. Starodumov[15], T. Susa

Institute Rudjer Boskovic, Zagreb, Croatia

A. Attikis, K. Christoforou, A. Hadjiagapiou, C. Leonidou, J. Mousa, C. Nicolaou, L. Paizanos, F. Ptochos, P.A. Razis, H. Rykaczewski, H. Saka, A. Stepennov

University of Cyprus, Nicosia, Cyprus

M. Finger, M. Finger Jr., A. Kveton

Charles University, Prague, Czech Republic

E. Ayala

Escuela Politecnica Nacional, Quito, Ecuador

E. Carrera Jarrin

Universidad San Francisco de Quito, Quito, Ecuador

A.A. Abdelalim[16,17], S. Elgammal[18], A. Ellithi Kamel[19]

Academy of Scientific Research and Technology of the Arab Republic of Egypt, Egyptian Network of High Energy Physics, Cairo, Egypt

M.A. Mahmoud, Y. Mohammed

Center for High Energy Physics (CHEP-FU), Fayoum University, El-Fayoum, Egypt

K. Ehataht, M. Kadastik, T. Lange, S. Nandan, C. Nielsen, J. Pata, M. Raidal, L. Tani, C. Veelken

National Institute of Chemical Physics and Biophysics, Tallinn, Estonia

H. Kirschenmann, K. Osterberg, M. Voutilainen

Department of Physics, University of Helsinki, Helsinki, Finland

S. Bharthuar, N. Bin Norjoharuddeen, E. Brücken, F. Garcia, P. Inkaew, K.T.S. Kallonen, T. Lampén, K. Lassila-Perini, S. Lehti, T. Lindén, M. Myllymäki, M.m. Rantanen, H. Siikonen, J. Tuominiemi

Helsinki Institute of Physics, Helsinki, Finland

P. Luukka, H. Petrow

Lappeenranta-Lahti University of Technology, Lappeenranta, Finland

M. Besancon, F. Couderc, M. Dejardin, D. Denegri, J.L. Faure, F. Ferri, S. Ganjour, P. Gras, G. Hamel de Monchenault, M. Kumar, V. Lohezic, J. Malcles, F. Orlandi, L. Portales, A. Rosowsky, M.Ö. Sahin, A. Savoy-Navarro[20], P. Simkina, M. Titov, M. Tornago

IRFU, CEA, Université Paris-Saclay, Gif-sur-Yvette, France

F. Beaudette, G. Boldrini, P. Busson, A. Cappati, C. Charlot, M. Chiusi, F. Damas, O. Davignon, A. De Wit, I.T. Ehle, B.A. Fontana Santos Alves, S. Ghosh, A. Gilbert, R. Granier de Cassagnac, A. Hakimi, B. Harikrishnan, L. Kalipoliti, G. Liu, M. Nguyen, C. Ochando, R. Salerno, J.B. Sauvan, Y. Sirois, L. Urda Gómez, E. Vernazza, A. Zabi, A. Zghiche

Laboratoire Leprince-Ringuet, CNRS/IN2P3, Ecole Polytechnique, Institut Polytechnique de Paris, Palaiseau, France

J.-L. Agram[21], J. Andrea, D. Apparu, D. Bloch, J.-M. Brom, E.C. Chabert, C. Collard, S. Falke, U. Goerlach, R. Haeberle, A.-C. Le Bihan, M. Meena, O. Poncet, G. Saha, M.A. Sessini, P. Van Hove, P. Vaucelle

Université de Strasbourg, CNRS, IPHC UMR 7178, Strasbourg, France

A. Di Florio

Centre de Calcul de l'Institut National de Physique Nucleaire et de Physique des Particules, CNRS/IN2P3, Villeurbanne, France

D. Amram, S. Beauceron, B. Blancon, G. Boudoul, N. Chanon, D. Contardo, P. Depasse, C. Dozen[22], H. El Mamouni, J. Fay, S. Gascon, M. Gouzevitch, C. Greenberg, G. Grenier, B. Ille, E. Jourd'huy, I.B. Laktineh, M. Lethuillier, L. Mirabito, S. Perries, A. Purohit, M. Vander Donckt, P. Verdier, J. Xiao

Institut de Physique des 2 Infinis de Lyon (IP2I), Villeurbanne, France

I. Lomidze, T. Toriashvili[23], Z. Tsamalaidze[15]

Georgian Technical University, Tbilisi, Georgia

V. Botta, S. Consuegra Rodríguez, L. Feld, K. Klein, M. Lipinski, D. Meuser, A. Pauls, D. Pérez Adán, N. Röwert, M. Teroerde

RWTH Aachen University, I. Physikalisches Institut, Aachen, Germany

S. Diekmann, A. Dodonova, N. Eich, D. Eliseev, F. Engelke, J. Erdmann, M. Erdmann, P. Fackeldey, B. Fischer, T. Hebbeker, K. Hoepfner, F. Ivone, A. Jung, M.y. Lee, F. Mausolf, M. Merschmeyer, A. Meyer, S. Mukherjee, D. Noll, F. Nowotny, A. Pozdnyakov, Y. Rath, W. Redjeb, F. Rehm, H. Reithler, V. Sarkisovi, A. Schmidt, C. Seth, A. Sharma, J.L. Spah, A. Stein, F. Torres Da Silva De Araujo[24], S. Wiedenbeck, S. Zaleski

RWTH Aachen University, III. Physikalisches Institut A, Aachen, Germany

C. Dziwok, G. Flügge, T. Kress, A. Nowack, O. Pooth, A. Stahl, T. Ziemons, A. Zotz

RWTH Aachen University, III. Physikalisches Institut B, Aachen, Germany

H. Aarup Petersen, M. Aldaya Martin, J. Alimena, S. Amoroso, Y. An, J. Bach, S. Baxter, M. Bayatmakou, H. Becerril Gonzalez, O. Behnke, A. Belvedere, F. Blekman[25], K. Borras[26], A. Campbell, A. Cardini, C. Cheng, F. Colombina, G. Eckerlin, D. Eckstein, L.I. Estevez Banos, O. Filatov, E. Gallo[25], A. Geiser, V. Guglielmi, M. Guthoff, A. Hinzmann, L. Jeppe, B. Kaech, M. Kasemann, C. Kleinwort, R. Kogler, M. Komm, D. Krücker, W. Lange, D. Leyva Pernia, K. Lipka[27], W. Lohmann[28], F. Lorkowski, R. Mankel, I.-A. Melzer-Pellmann, M. Mendizabal Morentin, A.B. Meyer, G. Milella, K. Moral Figueroa, A. Mussgiller, L.P. Nair, J. Niedziela, A. Nürnberg, Y. Otarid, J. Park, E. Ranken, A. Raspereza, D. Rastorguev, J. Rübenach, L. Rygaard, A. Saggio, M. Scham[29,26], S. Schnake[26], P. Schütze, C. Schwanenberger[25], D. Selivanova, K. Sharko, M. Shchedrolosiev, D. Stafford, F. Vazzoler, A. Ventura Barroso, R. Walsh, D. Wang, Q. Wang, Y. Wen, K. Wichmann, L. Wiens[26], C. Wissing, Y. Yang, A. Zimermmane Castro Santos

Deutsches Elektronen-Synchrotron, Hamburg, Germany

A. Albrecht, S. Albrecht, M. Antonello, S. Bein, L. Benato, S. Bollweg, M. Bonanomi, P. Connor, K. El Morabit, Y. Fischer, E. Garutti, A. Grohsjean, J. Haller, H.R. Jabusch, G. Kasieczka, P. Keicher, R. Klanner, W. Korcari, T. Kramer, C.c. Kuo, V. Kutzner, F. Labe, J. Lange, A. Lobanov, C. Matthies, L. Moureaux, M. Mrowietz, A. Nigamova, Y. Nissan, A. Paasch, K.J. Pena Rodriguez, T. Quadfasel, B. Raciti, M. Rieger, D. Savoiu, J. Schindler, P. Schleper, M. Schröder, J. Schwandt, M. Sommerhalder, H. Stadie, G. Steinbrück, A. Tews, M. Wolf

University of Hamburg, Hamburg, Germany

S. Brommer, M. Burkart, E. Butz, T. Chwalek, A. Dierlamm, A. Droll, U. Elicabuk, N. Faltermann, M. Giffels, A. Gottmann, F. Hartmann [30], R. Hofsaess, M. Horzela, U. Husemann, J. Kieseler, M. Klute, R. Koppenhöfer, J.M. Lawhorn, M. Link, A. Lintuluoto, S. Maier, S. Mitra, M. Mormile, Th. Müller, M. Neukum, M. Oh, E. Pfeffer, M. Presilla, G. Quast, K. Rabbertz, B. Regnery, N. Shadskiy, I. Shvetsov, H.J. Simonis, L. Sowa, L. Stockmeier, K. Tauqeer, M. Toms, N. Trevisani, R.F. Von Cube, M. Wassmer, S. Wieland, F. Wittig, R. Wolf, X. Zuo

Karlsruher Institut fuer Technologie, Karlsruhe, Germany

G. Anagnostou, G. Daskalakis, A. Kyriakis, A. Papadopoulos [30], A. Stakia

Institute of Nuclear and Particle Physics (INPP), NCSR Demokritos, Aghia Paraskevi, Greece

P. Kontaxakis, G. Melachroinos, Z. Painesis, I. Papavergou, I. Paraskevas, N. Saoulidou, K. Theofilatos, E. Tziaferi, K. Vellidis, I. Zisopoulos

National and Kapodistrian University of Athens, Athens, Greece

G. Bakas, T. Chatzistavrou, G. Karapostoli, K. Kousouris, I. Papakrivopoulos, E. Siamarkou, G. Tsipolitis, A. Zacharopoulou

National Technical University of Athens, Athens, Greece

K. Adamidis, I. Bestintzanos, I. Evangelou, C. Foudas, C. Kamtsikis, P. Katsoulis, P. Kokkas, P.G. Kosmoglou Kioseoglou, N. Manthos, I. Papadopoulos, J. Strologas

University of Ioánnina, Ioánnina, Greece

C. Hajdu, D. Horvath [31,32], K. Márton, A.J. Rádl [33], F. Sikler, V. Veszpremi

HUN-REN Wigner Research Centre for Physics, Budapest, Hungary

M. Csanád, K. Farkas, A. Fehérkuti [34], M.M.A. Gadallah [35], Á. Kadlecsik, P. Major, G. Pásztor, G.I. Veres

MTA-ELTE Lendület CMS Particle and Nuclear Physics Group, Eötvös Loránd University, Budapest, Hungary

B. Ujvari, G. Zilizi

Faculty of Informatics, University of Debrecen, Debrecen, Hungary

G. Bencze, S. Czellar, J. Molnar, Z. Szillasi

HUN-REN ATOMKI - Institute of Nuclear Research, Debrecen, Hungary

T. Csorgo [34], F. Nemes [34], T. Novak

Karoly Robert Campus, MATE Institute of Technology, Gyongyos, Hungary

S. Bansal, S.B. Beri, V. Bhatnagar, G. Chaudhary, S. Chauhan, N. Dhingra [36], A. Kaur, A. Kaur, H. Kaur, M. Kaur, S. Kumar, T. Sheokand, J.B. Singh, A. Singla

Panjab University, Chandigarh, India

A. Ahmed, A. Bhardwaj, A. Chhetri, B.C. Choudhary, A. Kumar, A. Kumar, M. Naimuddin, K. Ranjan, M.K. Saini, S. Saumya

University of Delhi, Delhi, India

S. Baradia, S. Barman [37], S. Bhattacharya, S. Das Gupta, S. Dutta, S. Dutta, S. Sarkar

Saha Institute of Nuclear Physics, HBNI, Kolkata, India

M.M. Ameen, P.K. Behera, S.C. Behera, S. Chatterjee, G. Dash, P. Jana, P. Kalbhor, S. Kamble, J.R. Komaragiri[38], D. Kumar[38], T. Mishra, B. Parida, P.R. Pujahari, N.R. Saha, A. Sharma, A.K. Sikdar, R.K. Singh, P. Verma, S. Verma, A. Vijay

Indian Institute of Technology Madras, Madras, India

S. Dugad, G.B. Mohanty, M. Shelake, P. Suryadevara

Tata Institute of Fundamental Research-A, Mumbai, India

A. Bala, S. Banerjee, R.M. Chatterjee, M. Guchait, Sh. Jain, A. Jaiswal, S. Kumar, G. Majumder, K. Mazumdar, S. Parolia, A. Thachayath

Tata Institute of Fundamental Research-B, Mumbai, India

S. Bahinipati[39], C. Kar, D. Maity[40], P. Mal, V.K. Muraleedharan Nair Bindhu[40], K. Naskar[40], A. Nayak[40], S. Nayak, K. Pal, P. Sadangi, S.K. Swain, S. Varghese[40], D. Vats[40]

National Institute of Science Education and Research, An OCC of Homi Bhabha National Institute, Bhubaneswar, Odisha, India

S. Acharya[41], A. Alpana, S. Dube, B. Gomber[41], P. Hazarika, B. Kansal, A. Laha, B. Sahu[41], S. Sharma, K.Y. Vaish

Indian Institute of Science Education and Research (IISER), Pune, India

H. Bakhshiansohi[42], A. Jafari[43], M. Zeinali[44]

Isfahan University of Technology, Isfahan, Iran

S. Bashiri, S. Chenarani[45], S.M. Etesami, Y. Hosseini, M. Khakzad, E. Khazaie, M. Mohammadi Najafabadi, S. Tizchang[46]

Institute for Research in Fundamental Sciences (IPM), Tehran, Iran

M. Felcini, M. Grunewald

University College Dublin, Dublin, Ireland

M. Abbrescia[a,b], A. Colaleo[a,b], D. Creanza[a,c], B. D'Anzi[a,b], N. De Filippis[a,c], M. De Palma[a,b], W. Elmetenawee[a,b,16], L. Fiore[a], G. Iaselli[a,c], L. Longo[a], M. Louka[a,b], G. Maggi[a,c], M. Maggi[a], I. Margjeka[a], V. Mastrapasqua[a,b], S. My[a,b], S. Nuzzo[a,b], A. Pellecchia[a,b], A. Pompili[a,b], G. Pugliese[a,c], R. Radogna[a,b], D. Ramos[a], A. Ranieri[a], L. Silvestris[a], F.M. Simone[a,c], Ü. Sözbilir[a], A. Stamerra[a,b], D. Troiano[a,b], R. Venditti[a,b], P. Verwilligen[a], A. Zaza[a,b]

[a] *INFN Sezione di Bari, Bari, Italy*
[b] *Università di Bari, Bari, Italy*
[c] *Politecnico di Bari, Bari, Italy*

G. Abbiendi[a], C. Battilana[a,b], D. Bonacorsi[a,b], P. Capiluppi[a,b], A. Castro[a,b,†], F.R. Cavallo[a], M. Cuffiani[a,b], G.M. Dallavalle[a], T. Diotalevi[a,b], F. Fabbri[a], A. Fanfani[a,b], D. Fasanella[a], P. Giacomelli[a], L. Giommi[a,b], C. Grandi[a], L. Guiducci[a,b], S. Lo Meo[a,47], M. Lorusso[a,b], L. Lunerti[a], S. Marcellini[a], G. Masetti[a], F.L. Navarria[a,b], G. Paggi[a,b], A. Perrotta[a], F. Primavera[a,b], A.M. Rossi[a,b], S. Rossi Tisbeni[a,b], T. Rovelli[a,b], G.P. Siroli[a,b]

[a] *INFN Sezione di Bologna, Bologna, Italy*
[b] *Università di Bologna, Bologna, Italy*

S. Costa[a,b,48], A. Di Mattia[a], A. Lapertosa[a], R. Potenza[a,b], A. Tricomi[a,b,48], C. Tuve[a,b]

[a] *INFN Sezione di Catania, Catania, Italy*
[b] *Università di Catania, Catania, Italy*

P. Assiouras [a], G. Barbagli [a], G. Bardelli [a,b], B. Camaiani [a,b], A. Cassese [a], R. Ceccarelli [a], V. Ciulli [a,b], C. Civinini [a], R. D'Alessandro [a,b], E. Focardi [a,b], T. Kello [a], G. Latino [a,b], P. Lenzi [a,b], M. Lizzo [a], M. Meschini [a], S. Paoletti [a], A. Papanastassiou [a,b], G. Sguazzoni [a], L. Viliani [a]

[a] *INFN Sezione di Firenze, Firenze, Italy*
[b] *Università di Firenze, Firenze, Italy*

L. Benussi, S. Bianco, S. Meola [49], D. Piccolo

INFN Laboratori Nazionali di Frascati, Frascati, Italy

P. Chatagnon [a], F. Ferro [a], E. Robutti [a], S. Tosi [a,b]

[a] *INFN Sezione di Genova, Genova, Italy*
[b] *Università di Genova, Genova, Italy*

A. Benaglia [a], F. Brivio [a], F. Cetorelli [a,b], F. De Guio [a,b], M.E. Dinardo [a,b], P. Dini [a], S. Gennai [a], R. Gerosa [a,b], A. Ghezzi [a,b], P. Govoni [a,b], L. Guzzi [a], M.T. Lucchini [a,b], M. Malberti [a], S. Malvezzi [a], A. Massironi [a], D. Menasce [a], L. Moroni [a], M. Paganoni [a,b], S. Palluotto [a,b], D. Pedrini [a], A. Perego [a,b], B.S. Pinolini [a], G. Pizzati [a,b], S. Ragazzi [a,b], T. Tabarelli de Fatis [a,b]

[a] *INFN Sezione di Milano-Bicocca, Milano, Italy*
[b] *Università di Milano-Bicocca, Milano, Italy*

S. Buontempo [a], A. Cagnotta [a,b], F. Carnevali [a,b], N. Cavallo [a,c], F. Fabozzi [a,c], A.O.M. Iorio [a,b], L. Lista [a,b,50], P. Paolucci [a,30], B. Rossi [a]

[a] *INFN Sezione di Napoli, Napoli, Italy*
[b] *Università di Napoli 'Federico II', Napoli, Italy*
[c] *Università della Basilicata, Potenza, Italy*
[d] *Scuola Superiore Meridionale (SSM), Napoli, Italy*

R. Ardino [a], P. Azzi [a], N. Bacchetta [a,51], D. Bisello [a,b], P. Bortignon [a], G. Bortolato [a,b], A. Bragagnolo [a,b], A.C.M. Bulla [a], R. Carlin [a,b], P. Checchia [a], T. Dorigo [a], F. Gasparini [a,b], U. Gasparini [a,b], S. Giorgetti [a], E. Lusiani [a], M. Margoni [a,b], A.T. Meneguzzo [a,b], M. Migliorini [a,b], F. Montecassiano [a], J. Pazzini [a,b], P. Ronchese [a,b], R. Rossin [a,b], F. Simonetto [a,b], M. Tosi [a,b], A. Triossi [a,b], S. Ventura [a], P. Zotto [a,b], A. Zucchetta [a,b], G. Zumerle [a,b]

[a] *INFN Sezione di Padova, Padova, Italy*
[b] *Università di Padova, Padova, Italy*
[c] *Università di Trento, Trento, Italy*

A. Braghieri [a], S. Calzaferri [a], D. Fiorina [a], P. Montagna [a,b], V. Re [a], C. Riccardi [a,b], P. Salvini [a], I. Vai [a,b], P. Vitulo [a,b]

[a] *INFN Sezione di Pavia, Pavia, Italy*
[b] *Università di Pavia, Pavia, Italy*

S. Ajmal [a,b], M.E. Ascioti [a,b], G.M. Bilei [a], C. Carrivale [a,b], D. Ciangottini [a,b], L. Fanò [a,b], M. Magherini [a,b], V. Mariani [a,b], M. Menichelli [a], F. Moscatelli [a,52], A. Rossi [a,b], A. Santocchia [a,b], D. Spiga [a], T. Tedeschi [a,b]

[a] *INFN Sezione di Perugia, Perugia, Italy*
[b] *Università di Perugia, Perugia, Italy*

C. Aimè [a], C.A. Alexe [a,c], P. Asenov [a,b], P. Azzurri [a], G. Bagliesi [a], R. Bhattacharya [a], L. Bianchini [a,b], T. Boccali [a], E. Bossini [a], D. Bruschini [a,c], R. Castaldi [a], M.A. Ciocci [a,b], M. Cipriani [a,b], V. D'Amante [a,d], R. Dell'Orso [a], S. Donato [a], A. Giassi [a], F. Ligabue [a,c], A.C. Marini [a], D. Matos Figueiredo [a], A. Messineo [a,b], S. Mishra [a], M. Musich [a,b], F. Palla [a], A. Rizzi [a,b], G. Rolandi [a,c], S. Roy Chowdhury [a], T. Sarkar [a], A. Scribano [a], P. Spagnolo [a], R. Tenchini [a], G. Tonelli [a,b], N. Turini [a,d], F. Vaselli [a,c], A. Venturi [a], P.G. Verdini [a]

[a] INFN Sezione di Pisa, Pisa, Italy
[b] Università di Pisa, Pisa, Italy
[c] Scuola Normale Superiore di Pisa, Pisa, Italy
[d] Università di Siena, Siena, Italy

C. Baldenegro Barrera [a,b], P. Barria [a], C. Basile [a,b], F. Cavallari [a], L. Cunqueiro Mendez [a,b], D. Del Re [a,b], E. Di Marco [a,b], M. Diemoz [a], F. Errico [a,b], R. Gargiulo [a,b], E. Longo [a,b], L. Martikainen [a,b], J. Mijuskovic [a,b], G. Organtini [a,b], F. Pandolfi [a], R. Paramatti [a,b], C. Quaranta [a,b], S. Rahatlou [a,b], C. Rovelli [a], F. Santanastasio [a,b], L. Soffi [a]

[a] INFN Sezione di Roma, Roma, Italy
[b] Sapienza Università di Roma, Roma, Italy

N. Amapane [a,b], R. Arcidiacono [a,c], S. Argiro [a,b], M. Arneodo [a,c], N. Bartosik [a], R. Bellan [a,b], A. Bellora [a,b], C. Biino [a], C. Borca [a,b], N. Cartiglia [a], M. Costa [a,b], R. Covarelli [a,b], N. Demaria [a], L. Finco [a], M. Grippo [a,b], B. Kiani [a,b], F. Legger [a], F. Luongo [a,b], C. Mariotti [a], L. Markovic [a,b], S. Maselli [a], A. Mecca [a,b], L. Menzio [a,b], P. Meridiani [a], E. Migliore [a,b], M. Monteno [a], R. Mulargia [a], M.M. Obertino [a,b], G. Ortona [a], L. Pacher [a,b], N. Pastrone [a], M. Pelliccioni [a], M. Ruspa [a,c], F. Siviero [a,b], V. Sola [a,b], A. Solano [a,b], A. Staiano [a], C. Tarricone [a,b], D. Trocino [a], G. Umoret [a,b], R. White [a,b]

[a] INFN Sezione di Torino, Torino, Italy
[b] Università di Torino, Torino, Italy
[c] Università del Piemonte Orientale, Novara, Italy

J. Babbar [a,b], S. Belforte [a], V. Candelise [a,b], M. Casarsa [a], F. Cossutti [a], K. De Leo [a], G. Della Ricca [a,b]

[a] INFN Sezione di Trieste, Trieste, Italy
[b] Università di Trieste, Trieste, Italy

S. Dogra, J. Hong, B. Kim, J. Kim, D. Lee, H. Lee, S.W. Lee, C.S. Moon, Y.D. Oh, M.S. Ryu, S. Sekmen, B. Tae, Y.C. Yang

Kyungpook National University, Daegu, Korea

M.S. Kim

Department of Mathematics and Physics - GWNU, Gangneung, Korea

G. Bak, P. Gwak, H. Kim, D.H. Moon

Chonnam National University, Institute for Universe and Elementary Particles, Kwangju, Korea

E. Asilar, J. Choi, D. Kim, T.J. Kim, J.A. Merlin, Y. Ryou

Hanyang University, Seoul, Korea

S. Choi, S. Han, B. Hong, K. Lee, K.S. Lee, S. Lee, J. Yoo

Korea University, Seoul, Korea

J. Goh, S. Yang

Kyung Hee University, Department of Physics, Seoul, Korea

H.S. Kim, Y. Kim, S. Lee

Sejong University, Seoul, Korea

J. Almond, J.H. Bhyun, J. Choi, J. Choi, W. Jun, J. Kim, Y.W. Kim, S. Ko, H. Kwon, H. Lee, J. Lee, J. Lee, B.H. Oh, S.B. Oh, H. Seo, U.K. Yang, I. Yoon

Seoul National University, Seoul, Korea

W. Jang, D.Y. Kang, Y. Kang, S. Kim, B. Ko, J.S.H. Lee, Y. Lee, I.C. Park, Y. Roh, I.J. Watson

University of Seoul, Seoul, Korea

S. Ha, K. Hwang, H.D. Yoo

Yonsei University, Department of Physics, Seoul, Korea

M. Choi, M.R. Kim, H. Lee, Y. Lee, I. Yu

Sungkyunkwan University, Suwon, Korea

T. Beyrouthy, Y. Gharbia

College of Engineering and Technology, American University of the Middle East (AUM), Dasman, Kuwait

F. Alazemi

Kuwait University - College of Science - Department of Physics, Safat, Kuwait

K. Dreimanis, A. Gaile, C. Munoz Diaz, D. Osite, G. Pikurs, A. Potrebko, M. Seidel, D. Sidiropoulos Kontos

Riga Technical University, Riga, Latvia

N.R. Strautnieks

University of Latvia (LU), Riga, Latvia

M. Ambrozas, A. Juodagalvis, A. Rinkevicius, G. Tamulaitis

Vilnius University, Vilnius, Lithuania

I. Yusuff[53], Z. Zolkapli

National Centre for Particle Physics, Universiti Malaya, Kuala Lumpur, Malaysia

J.F. Benitez, A. Castaneda Hernandez, H.A. Encinas Acosta, L.G. Gallegos Maríñez, M. León Coello, J.A. Murillo Quijada, A. Sehrawat, L. Valencia Palomo

Universidad de Sonora (UNISON), Hermosillo, Mexico

G. Ayala, H. Castilla-Valdez, H. Crotte Ledesma, E. De La Cruz-Burelo, I. Heredia-De La Cruz[54], R. Lopez-Fernandez, J. Mejia Guisao, C.A. Mondragon Herrera, A. Sánchez Hernández

Centro de Investigacion y de Estudios Avanzados del IPN, Mexico City, Mexico

C. Oropeza Barrera, D.L. Ramirez Guadarrama, M. Ramírez García

Universidad Iberoamericana, Mexico City, Mexico

I. Bautista, I. Pedraza, H.A. Salazar Ibarguen, C. Uribe Estrada

Benemerita Universidad Autonoma de Puebla, Puebla, Mexico

I. Bubanja, N. Raicevic

University of Montenegro, Podgorica, Montenegro

P.H. Butler

University of Canterbury, Christchurch, New Zealand

A. Ahmad, M.I. Asghar, A. Awais, M.I.M. Awan, H.R. Hoorani, W.A. Khan

National Centre for Physics, Quaid-I-Azam University, Islamabad, Pakistan

V. Avati, L. Grzanka, M. Malawski

AGH University of Krakow, Krakow, Poland

H. Bialkowska, M. Bluj, M. Górski, M. Kazana, M. Szleper, P. Zalewski

National Centre for Nuclear Research, Swierk, Poland

K. Bunkowski, K. Doroba, A. Kalinowski, M. Konecki, J. Krolikowski, A. Muhammad

Institute of Experimental Physics, Faculty of Physics, University of Warsaw, Warsaw, Poland

K. Pozniak, W. Zabolotny

Warsaw University of Technology, Warsaw, Poland

M. Araujo, D. Bastos, C. Beirão Da Cruz E Silva, A. Boletti, M. Bozzo, T. Camporesi, G. Da Molin, P. Faccioli, M. Gallinaro, J. Hollar, N. Leonardo, G.B. Marozzo, T. Niknejad, A. Petrilli, M. Pisano, J. Seixas, J. Varela, J.W. Wulff

Laboratório de Instrumentação e Física Experimental de Partículas, Lisboa, Portugal

P. Adzic, P. Milenovic

Faculty of Physics, University of Belgrade, Belgrade, Serbia

D. Devetak, M. Dordevic, J. Milosevic, L. Nadderd, V. Rekovic

VINCA Institute of Nuclear Sciences, University of Belgrade, Belgrade, Serbia

J. Alcaraz Maestre, Cristina F. Bedoya, J.A. Brochero Cifuentes, Oliver M. Carretero, M. Cepeda, M. Cerrada, N. Colino, B. De La Cruz, A. Delgado Peris, A. Escalante Del Valle, D. Fernández Del Val, J.P. Fernández Ramos, J. Flix, M.C. Fouz, O. Gonzalez Lopez, S. Goy Lopez, J.M. Hernandez, M.I. Josa, J. Llorente Merino, E. Martin Viscasillas, D. Moran, C.M. Morcillo Perez, Á. Navarro Tobar, C. Perez Dengra, A. Pérez-Calero Yzquierdo, J. Puerta Pelayo, I. Redondo, S. Sánchez Navas, J. Sastre, J. Vazquez Escobar

Centro de Investigaciones Energéticas Medioambientales y Tecnológicas (CIEMAT), Madrid, Spain

J.F. de Trocóniz

Universidad Autónoma de Madrid, Madrid, Spain

B. Alvarez Gonzalez, J. Cuevas, J. Fernandez Menendez, S. Folgueras, I. Gonzalez Caballero, P. Leguina, E. Palencia Cortezon, J. Prado Pico, C. Ramón Álvarez, V. Rodríguez Bouza, A. Soto Rodríguez, A. Trapote, C. Vico Villalba, P. Vischia

Universidad de Oviedo, Instituto Universitario de Ciencias y Tecnologías Espaciales de Asturias (ICTEA), Oviedo, Spain

S. Bhowmik, S. Blanco Fernández, I.J. Cabrillo, A. Calderon, J. Duarte Campderros, M. Fernandez, G. Gomez, C. Lasaosa García, R. Lopez Ruiz, C. Martinez Rivero, P. Martinez Ruiz del Arbol, F. Matorras, P. Matorras Cuevas, E. Navarrete Ramos, J. Piedra Gomez, L. Scodellaro, I. Vila, J.M. Vizan Garcia

Instituto de Física de Cantabria (IFCA), CSIC-Universidad de Cantabria, Santander, Spain

B. Kailasapathy[55], D.D.C. Wickramarathna

University of Colombo, Colombo, Sri Lanka

W.G.D. Dharmaratna[56], K. Liyanage, N. Perera

University of Ruhuna, Department of Physics, Matara, Sri Lanka

D. Abbaneo, C. Amendola, E. Auffray, G. Auzinger, J. Baechler, D. Barney, A. Bermúdez Martínez, M. Bianco, A.A. Bin Anuar, A. Bocci, L. Borgonovi, C. Botta, E. Brondolin, C. Caillol, G. Cerminara, N. Chernyavskaya, D. d'Enterria, A. Dabrowski, A. David, A. De Roeck, M.M. Defranchis, M. Deile, M. Dobson, G. Franzoni, W. Funk, S. Giani, D. Gigi, K. Gill, F. Glege, J. Hegeman, J.K. Heikkilä, B. Huber, V. Innocente, T. James, P. Janot, O. Kaluzinska, O. Karacheban[28], S. Laurila, P. Lecoq, E. Leutgeb, C. Lourenço,

L. Malgeri, M. Mannelli, M. Matthewman, A. Mehta, F. Meijers, S. Mersi, E. Meschi, V. Milosevic, F. Monti, F. Moortgat, M. Mulders, I. Neutelings, S. Orfanelli, F. Pantaleo, G. Petrucciani, A. Pfeiffer, M. Pierini, H. Qu, D. Rabady, B. Ribeiro Lopes, M. Rovere, H. Sakulin, S. Sanchez Cruz, S. Scarfi, C. Schwick, M. Selvaggi, A. Sharma, K. Shchelina, P. Silva, P. Sphicas [57], A.G. Stahl Leiton, A. Steen, S. Summers, D. Treille, P. Tropea, D. Walter, J. Wanczyk [58], J. Wang, K.A. Wozniak [59], S. Wuchterl, P. Zehetner, P. Zejdl, W.D. Zeuner

CERN, European Organization for Nuclear Research, Geneva, Switzerland

T. Bevilacqua [60], L. Caminada [60], A. Ebrahimi, W. Erdmann, R. Horisberger, Q. Ingram, H.C. Kaestli, D. Kotlinski, C. Lange, M. Missiroli [60], L. Noehte [60], T. Rohe, A. Samalan

Paul Scherrer Institut, Villigen, Switzerland

T.K. Aarrestad, M. Backhaus, G. Bonomelli, A. Calandri, C. Cazzaniga, K. Datta, P. De Bryas Dexmiers D'archiac [58], A. De Cosa, G. Dissertori, M. Dittmar, M. Donegà, F. Eble, M. Galli, K. Gedia, F. Glessgen, C. Grab, N. Härringer, T.G. Harte, D. Hits, W. Lustermann, A.-M. Lyon, R.A. Manzoni, M. Marchegiani, L. Marchese, C. Martin Perez, A. Mascellani [58], F. Nessi-Tedaldi, F. Pauss, V. Perovic, S. Pigazzini, B. Ristic, F. Riti, R. Seidita, J. Steggemann [58], A. Tarabini, D. Valsecchi, R. Wallny

ETH Zurich - Institute for Particle Physics and Astrophysics (IPA), Zurich, Switzerland

C. Amsler [61], P. Bärtschi, M.F. Canelli, K. Cormier, M. Huwiler, W. Jin, A. Jofrehei, B. Kilminster, S. Leontsinis, S.P. Liechti, A. Macchiolo, P. Meiring, F. Meng, U. Molinatti, J. Motta, A. Reimers, P. Robmann, M. Senger, E. Shokr, F. Stäger, R. Tramontano

Universität Zürich, Zurich, Switzerland

C. Adloff [62], D. Bhowmik, C.M. Kuo, W. Lin, P.K. Rout, P.C. Tiwari [38], S.S. Yu

National Central University, Chung-Li, Taiwan

L. Ceard, K.F. Chen, P.s. Chen, Z.g. Chen, A. De Iorio, W.-S. Hou, T.h. Hsu, Y.w. Kao, S. Karmakar, G. Kole, Y.y. Li, R.-S. Lu, E. Paganis, X.f. Su, J. Thomas-Wilsker, L.s. Tsai, D. Tsionou, H.y. Wu, E. Yazgan

National Taiwan University (NTU), Taipei, Taiwan

C. Asawatangtrakuldee, N. Srimanobhas, V. Wachirapusitanand

High Energy Physics Research Unit, Department of Physics, Faculty of Science, Chulalongkorn University, Bangkok, Thailand

D. Agyel, F. Boran, F. Dolek, I. Dumanoglu [63], E. Eskut, Y. Guler [64], E. Gurpinar Guler [64], C. Isik, O. Kara, A. Kayis Topaksu, U. Kiminsu, Y. Komurcu, G. Onengut, K. Ozdemir [65], A. Polatoz, B. Tali [66], U.G. Tok, S. Turkcapar, E. Uslan, I.S. Zorbakir

Çukurova University, Physics Department, Science and Art Faculty, Adana, Turkey

G. Sokmen, M. Yalvac [67]

Middle East Technical University, Physics Department, Ankara, Turkey

B. Akgun, I.O. Atakisi, E. Gülmez, M. Kaya [68], O. Kaya [69], S. Tekten [70]

Bogazici University, Istanbul, Turkey

A. Cakir, K. Cankocak [63,71], G.G. Dincer [63], S. Sen [72]

Istanbul Technical University, Istanbul, Turkey

O. Aydilek [73], B. Hacisahinoglu, I. Hos [74], B. Kaynak, S. Ozkorucuklu, O. Potok, H. Sert, C. Simsek, C. Zorbilmez

Istanbul University, Istanbul, Turkey

S. Cerci, B. Isildak [75], D. Sunar Cerci, T. Yetkin

Yildiz Technical University, Istanbul, Turkey

A. Boyaryntsev, B. Grynyov

Institute for Scintillation Materials of National Academy of Science of Ukraine, Kharkiv, Ukraine

L. Levchuk

National Science Centre, Kharkiv Institute of Physics and Technology, Kharkiv, Ukraine

D. Anthony, J.J. Brooke, A. Bundock, F. Bury, E. Clement, D. Cussans, H. Flacher, M. Glowacki, J. Goldstein, H.F. Heath, M.-L. Holmberg, L. Kreczko, S. Paramesvaran, L. Robertshaw, S. Seif El Nasr-Storey, V.J. Smith, N. Stylianou [76], K. Walkingshaw Pass

University of Bristol, Bristol, United Kingdom

A.H. Ball, K.W. Bell, A. Belyaev [77], C. Brew, R.M. Brown, D.J.A. Cockerill, C. Cooke, A. Elliot, K.V. Ellis, K. Harder, S. Harper, J. Linacre, K. Manolopoulos, D.M. Newbold, E. Olaiya, D. Petyt, T. Reis, A.R. Sahasransu, G. Salvi, T. Schuh, C.H. Shepherd-Themistocleous, I.R. Tomalin, K.C. Whalen, T. Williams

Rutherford Appleton Laboratory, Didcot, United Kingdom

I. Andreou, R. Bainbridge, P. Bloch, C.E. Brown, O. Buchmuller, V. Cacchio, C.A. Carrillo Montoya, G.S. Chahal [78], D. Colling, J.S. Dancu, I. Das, P. Dauncey, G. Davies, J. Davies, M. Della Negra, S. Fayer, G. Fedi, G. Hall, M.H. Hassanshahi, A. Howard, G. Iles, C.R. Knight, J. Langford, J. León Holgado, L. Lyons, A.-M. Magnan, B. Maier, S. Mallios, M. Mieskolainen, J. Nash [79], M. Pesaresi, P.B. Pradeep, B.C. Radburn-Smith, A. Richards, A. Rose, K. Savva, C. Seez, R. Shukla, A. Tapper, K. Uchida, G.P. Uttley, L.H. Vage, T. Virdee [30], M. Vojinovic, N. Wardle, D. Winterbottom

Imperial College, London, United Kingdom

J.E. Cole, A. Khan, P. Kyberd, I.D. Reid

Brunel University, Uxbridge, United Kingdom

S. Abdullin, A. Brinkerhoff, E. Collins, M.R. Darwish, J. Dittmann, K. Hatakeyama, J. Hiltbrand, B. McMaster, J. Samudio, S. Sawant, C. Sutantawibul, J. Wilson

Baylor University, Waco, TX, USA

R. Bartek, A. Dominguez, A.E. Simsek

Catholic University of America, Washington, DC, USA

B. Bam, A. Buchot Perraguin, R. Chudasama, S.I. Cooper, C. Crovella, S.V. Gleyzer, E. Pearson, C.U. Perez, P. Rumerio [80], E. Usai, R. Yi

The University of Alabama, Tuscaloosa, AL, USA

A. Akpinar, C. Cosby, G. De Castro, Z. Demiragli, C. Erice, C. Fangmeier, C. Fernandez Madrazo, E. Fontanesi, D. Gastler, F. Golf, S. Jeon, J. O'cain, I. Reed, J. Rohlf, K. Salyer, D. Sperka, D. Spitzbart, I. Suarez, A. Tsatsos, A.G. Zecchinelli

Boston University, Boston, MA, USA

G. Benelli, D. Cutts, L. Gouskos, M. Hadley, U. Heintz, J.M. Hogan[81], T. Kwon, G. Landsberg, K.T. Lau, D. Li, J. Luo, S. Mondal, N. Pervan, T. Russell, S. Sagir[82], X. Shen, F. Simpson, M. Stamenkovic, N. Venkatasubramanian, X. Yan

Brown University, Providence, RI, USA

S. Abbott, C. Brainerd, R. Breedon, H. Cai, M. Calderon De La Barca Sanchez, M. Chertok, M. Citron, J. Conway, P.T. Cox, R. Erbacher, F. Jensen, O. Kukral, G. Mocellin, M. Mulhearn, S. Ostrom, W. Wei, S. Yoo, F. Zhang

University of California, Davis, Davis, CA, USA

M. Bachtis, R. Cousins, A. Datta, G. Flores Avila, J. Hauser, M. Ignatenko, M.A. Iqbal, T. Lam, E. Manca, A. Nunez Del Prado, D. Saltzberg, V. Valuev

University of California, Los Angeles, CA, USA

R. Clare, J.W. Gary, M. Gordon, G. Hanson, W. Si

University of California, Riverside, Riverside, CA, USA

A. Aportela, A. Arora, J.G. Branson, S. Cittolin, S. Cooperstein, D. Diaz, J. Duarte, L. Giannini, Y. Gu, J. Guiang, R. Kansal, V. Krutelyov, R. Lee, J. Letts, M. Masciovecchio, F. Mokhtar, S. Mukherjee, M. Pieri, M. Quinnan, B.V. Sathia Narayanan, V. Sharma, M. Tadel, E. Vourliotis, F. Würthwein, Y. Xiang, A. Yagil

University of California, San Diego, La Jolla, CA, USA

A. Barzdukas, L. Brennan, C. Campagnari, K. Downham, C. Grieco, J. Incandela, J. Kim, A.J. Li, P. Masterson, H. Mei, J. Richman, S.N. Santpur, U. Sarica, R. Schmitz, F. Setti, J. Sheplock, D. Stuart, T.Á. Vámi, S. Wang, D. Zhang

University of California, Santa Barbara - Department of Physics, Santa Barbara, CA, USA

S. Bhattacharya, A. Bornheim, O. Cerri, A. Latorre, J. Mao, H.B. Newman, G. Reales Gutiérrez, M. Spiropulu, J.R. Vlimant, C. Wang, S. Xie, R.Y. Zhu

California Institute of Technology, Pasadena, CA, USA

J. Alison, S. An, P. Bryant, M. Cremonesi, V. Dutta, T. Ferguson, T.A. Gómez Espinosa, A. Harilal, A. Kallil Tharayil, C. Liu, T. Mudholkar, S. Murthy, P. Palit, K. Park, M. Paulini, A. Roberts, A. Sanchez, W. Terrill

Carnegie Mellon University, Pittsburgh, PA, USA

J.P. Cumalat, W.T. Ford, A. Hart, A. Hassani, G. Karathanasis, N. Manganelli, J. Pearkes, C. Savard, N. Schonbeck, K. Stenson, K.A. Ulmer, S.R. Wagner, N. Zipper, D. Zuolo

University of Colorado Boulder, Boulder, CO, USA

J. Alexander, S. Bright-Thonney, X. Chen, D.J. Cranshaw, J. Fan, X. Fan, S. Hogan, P. Kotamnives, J. Monroy, M. Oshiro, J.R. Patterson, M. Reid, A. Ryd, J. Thom, P. Wittich, R. Zou

Cornell University, Ithaca, NY, USA

M. Albrow, M. Alyari, O. Amram, G. Apollinari, A. Apresyan, L.A.T. Bauerdick, D. Berry, J. Berryhill, P.C. Bhat, K. Burkett, J.N. Butler, A. Canepa, G.B. Cerati, H.W.K. Cheung, F. Chlebana, G. Cummings, J. Dickinson, I. Dutta, V.D. Elvira, Y. Feng, J. Freeman, A. Gandrakota, Z. Gecse, L. Gray, D. Green, A. Grummer, S. Grünendahl, D. Guerrero,

O. Gutsche, R.M. Harris, R. Heller, T.C. Herwig, J. Hirschauer, B. Jayatilaka, S. Jindariani, M. Johnson, U. Joshi, T. Klijnsma, B. Klima, K.H.M. Kwok, S. Lammel, C. Lee, D. Lincoln, R. Lipton, T. Liu, C. Madrid, K. Maeshima, C. Mantilla, D. Mason, P. McBride, P. Merkel, S. Mrenna, S. Nahn, J. Ngadiuba, D. Noonan, S. Norberg, V. Papadimitriou, N. Pastika, K. Pedro, C. Pena[83], F. Ravera, A. Reinsvold Hall[84], L. Ristori, M. Safdari, E. Sexton-Kennedy, N. Smith, A. Soha, L. Spiegel, S. Stoynev, J. Strait, L. Taylor, S. Tkaczyk, N.V. Tran, L. Uplegger, E.W. Vaandering, I. Zoi

Fermi National Accelerator Laboratory, Batavia, IL, USA

C. Aruta, P. Avery, D. Bourilkov, P. Chang, V. Cherepanov, R.D. Field, C. Huh, E. Koenig, M. Kolosova, J. Konigsberg, A. Korytov, K. Matchev, N. Menendez, G. Mitselmakher, K. Mohrman, A. Muthirakalayil Madhu, N. Rawal, S. Rosenzweig, Y. Takahashi, J. Wang

University of Florida, Gainesville, FL, USA

T. Adams, A. Al Kadhim, A. Askew, S. Bower, V. Hagopian, R. Hashmi, R.S. Kim, S. Kim, T. Kolberg, G. Martinez, H. Prosper, P.R. Prova, M. Wulansatiti, R. Yohay, J. Zhang

Florida State University, Tallahassee, FL, USA

B. Alsufyani, M.M. Baarmand, S. Butalla, S. Das, T. Elkafrawy[85], M. Hohlmann, E. Yanes

Florida Institute of Technology, Melbourne, FL, USA

M.R. Adams, A. Baty, C. Bennett, R. Cavanaugh, R. Escobar Franco, O. Evdokimov, C.E. Gerber, M. Hawksworth, A. Hingrajiya, D.J. Hofman, J.h. Lee, D.S. Lemos, A.H. Merrit, C. Mills, S. Nanda, G. Oh, B. Ozek, D. Pilipovic, R. Pradhan, E. Prifti, T. Roy, S. Rudrabhatla, N. Singh, M.B. Tonjes, N. Varelas, M.A. Wadud, Z. Ye, J. Yoo

University of Illinois Chicago, Chicago, IL, USA

M. Alhusseini, D. Blend, K. Dilsiz[86], L. Emediato, G. Karaman, O.K. Köseyan, J.-P. Merlo, A. Mestvirishvili[87], O. Neogi, H. Ogul[88], Y. Onel, A. Penzo, C. Snyder, E. Tiras[89]

The University of Iowa, Iowa City, IA, USA

B. Blumenfeld, L. Corcodilos, J. Davis, A.V. Gritsan, L. Kang, S. Kyriacou, P. Maksimovic, M. Roguljic, J. Roskes, S. Sekhar, M. Swartz

Johns Hopkins University, Baltimore, MD, USA

A. Abreu, L.F. Alcerro Alcerro, J. Anguiano, S. Arteaga Escatel, P. Baringer, A. Bean, Z. Flowers, D. Grove, J. King, G. Krintiras, M. Lazarovits, C. Le Mahieu, J. Marquez, M. Murray, M. Nickel, M. Pitt, S. Popescu[90], C. Rogan, C. Royon, R. Salvatico, S. Sanders, C. Smith, G. Wilson

The University of Kansas, Lawrence, KS, USA

B. Allmond, R. Gujju Gurunadha, A. Ivanov, K. Kaadze, Y. Maravin, J. Natoli, D. Roy, G. Sorrentino

Kansas State University, Manhattan, KS, USA

A. Baden, A. Belloni, J. Bistany-riebman, Y.M. Chen, S.C. Eno, N.J. Hadley, S. Jabeen, R.G. Kellogg, T. Koeth, B. Kronheim, Y. Lai, S. Lascio, A.C. Mignerey, S. Nabili, C. Palmer, C. Papageorgakis, M.M. Paranjpe, E. Popova[91], A. Shevelev, L. Wang

University of Maryland, College Park, MD, USA

J. Bendavid, I.A. Cali, P.c. Chou, M. D'Alfonso, J. Eysermans, C. Freer, G. Gomez-Ceballos, M. Goncharov, G. Grosso, P. Harris, D. Hoang, D. Kovalskyi, J. Krupa, L. Lavezzo, Y.-J. Lee, K. Long, C. Mcginn, A. Novak, M.I. Park, C. Paus, C. Reissel, C. Roland, G. Roland, S. Rothman, G.S.F. Stephans, Z. Wang, B. Wyslouch, T.J. Yang, K. Yoon

Massachusetts Institute of Technology, Cambridge, MA, USA

B. Crossman, B.M. Joshi, C. Kapsiak, M. Krohn, D. Mahon, J. Mans, B. Marzocchi, M. Revering, R. Rusack, R. Saradhy, N. Strobbe

University of Minnesota, Minneapolis, MN, USA

K. Bloom, D.R. Claes, G. Haza, J. Hossain, C. Joo, I. Kravchenko, J.E. Siado, W. Tabb, A. Vagnerini, A. Wightman, F. Yan, D. Yu

University of Nebraska-Lincoln, Lincoln, NE, USA

H. Bandyopadhyay, L. Hay, H.w. Hsia, I. Iashvili, A. Kalogeropoulos, A. Kharchilava, M. Morris, D. Nguyen, J. Pekkanen, S. Rappoccio, H. Rejeb Sfar, A. Williams, P. Young

State University of New York at Buffalo, Buffalo, NY, USA

G. Alverson, E. Barberis, J. Bonilla, B. Bylsma, M. Campana, J. Dervan, Y. Haddad, Y. Han, I. Israr, A. Krishna, J. Li, M. Lu, G. Madigan, R. Mccarthy, D.M. Morse, V. Nguyen, T. Orimoto, A. Parker, L. Skinnari, D. Wood

Northeastern University, Boston, MA, USA

J. Bueghly, S. Dittmer, K.A. Hahn, Y. Liu, M. Mcginnis, Y. Miao, D.G. Monk, M.H. Schmitt, A. Taliercio, M. Velasco

Northwestern University, Evanston, IL, USA

G. Agarwal, R. Band, R. Bucci, S. Castells, A. Das, R. Goldouzian, M. Hildreth, K.W. Ho, K. Hurtado Anampa, T. Ivanov, C. Jessop, K. Lannon, J. Lawrence, N. Loukas, L. Lutton, J. Mariano, N. Marinelli, I. Mcalister, T. McCauley, C. Mcgrady, C. Moore, Y. Musienko[15], H. Nelson, M. Osherson, A. Piccinelli, R. Ruchti, A. Townsend, Y. Wan, M. Wayne, H. Yockey, M. Zarucki, L. Zygala

University of Notre Dame, Notre Dame, IN, USA

A. Basnet, M. Carrigan, L.S. Durkin, C. Hill, M. Joyce, M. Nunez Ornelas, K. Wei, B.L. Winer, B.R. Yates

The Ohio State University, Columbus, OH, USA

H. Bouchamaoui, K. Coldham, P. Das, G. Dezoort, P. Elmer, A. Frankenthal, B. Greenberg, N. Haubrich, K. Kennedy, G. Kopp, S. Kwan, D. Lange, A. Loeliger, D. Marlow, I. Ojalvo, J. Olsen, D. Stickland, C. Tully

Princeton University, Princeton, NJ, USA

S. Malik

University of Puerto Rico, Mayaguez, PR, USA

A.S. Bakshi, S. Chandra, R. Chawla, A. Gu, L. Gutay, M. Jones, A.W. Jung, A.M. Koshy, M. Liu, G. Negro, N. Neumeister, G. Paspalaki, S. Piperov, V. Scheurer, J.F. Schulte, M. Stojanovic, J. Thieman, A.K. Virdi, F. Wang, A. Wildridge, W. Xie, Y. Yao

Purdue University, West Lafayette, IN, USA

J. Dolen, N. Parashar, A. Pathak

Purdue University Northwest, Hammond, IN, USA

D. Acosta, T. Carnahan, K.M. Ecklund, P.J. Fernández Manteca, S. Freed, P. Gardner, F.J.M. Geurts, I. Krommydas, W. Li, J. Lin, O. Miguel Colin, B.P. Padley, R. Redjimi, J. Rotter, E. Yigitbasi, Y. Zhang

Rice University, Houston, TX, USA

A. Bodek, P. de Barbaro, R. Demina, J.L. Dulemba, A. Garcia-Bellido, O. Hindrichs, A. Khukhunaishvili, N. Parmar, P. Parygin[91], R. Taus

University of Rochester, Rochester, NY, USA

B. Chiarito, J.P. Chou, S.V. Clark, D. Gadkari, Y. Gershtein, E. Halkiadakis, M. Heindl, C. Houghton, D. Jaroslawski, S. Konstantinou, I. Laflotte, A. Lath, R. Montalvo, K. Nash, J. Reichert, H. Routray, P. Saha, S. Salur, S. Schnetzer, S. Somalwar, R. Stone, S.A. Thayil, S. Thomas, J. Vora, H. Wang

Rutgers, The State University of New Jersey, Piscataway, NJ, USA

D. Ally, A.G. Delannoy, S. Fiorendi, S. Higginbotham, T. Holmes, A.R. Kanuganti, N. Karunarathna, L. Lee, E. Nibigira, S. Spanier

University of Tennessee, Knoxville, TN, USA

D. Aebi, M. Ahmad, T. Akhter, K. Androsov[58], O. Bouhali[92], R. Eusebi, J. Gilmore, T. Huang, T. Kamon[93], H. Kim, S. Luo, R. Mueller, D. Overton, D. Rathjens, A. Safonov

Texas A&M University, College Station, TX, USA

N. Akchurin, J. Damgov, N. Gogate, V. Hegde, A. Hussain, Y. Kazhykarim, K. Lamichhane, S.W. Lee, A. Mankel, T. Peltola, I. Volobouev

Texas Tech University, Lubbock, TX, USA

E. Appelt, Y. Chen, S. Greene, A. Gurrola, W. Johns, R. Kunnawalkam Elayavalli, A. Melo, F. Romeo, P. Sheldon, S. Tuo, J. Velkovska, J. Viinikainen

Vanderbilt University, Nashville, TN, USA

B. Cardwell, H. Chung, B. Cox, J. Hakala, R. Hirosky, A. Ledovskoy, C. Neu

University of Virginia, Charlottesville, VA, USA

S. Bhattacharya, P.E. Karchin

Wayne State University, Detroit, MI, USA

A. Aravind, S. Banerjee, K. Black, T. Bose, E. Chavez, S. Dasu, I. De Bruyn, P. Everaerts, C. Galloni, H. He, M. Herndon, A. Herve, C.K. Koraka, A. Lanaro, R. Loveless, J. Madhusudanan Sreekala, A. Mallampalli, A. Mohammadi, S. Mondal, G. Parida, L. Pétré, D. Pinna, A. Savin, V. Shang, V. Sharma, W.H. Smith, D. Teague, H.F. Tsoi, W. Vetens, A. Warden

University of Wisconsin - Madison, Madison, WI, USA

S. Afanasiev, V. Alexakhin, D. Budkouski, I. Golutvin[†], I. Gorbunov, V. Karjavine, V. Korenkov, A. Lanev, A. Malakhov, V. Matveev[94], V. Palichik, V. Perelygin, M. Savina, V. Shalaev, S. Shmatov, S. Shulha, V. Smirnov, O. Teryaev, N. Voytishin, B.S. Yuldashev[95], A. Zarubin, I. Zhizhin, G. Gavrilov, V. Golovtcov, Y. Ivanov, V. Kim[94], P. Levchenko[96], V. Murzin, V. Oreshkin, D. Sosnov, V. Sulimov, L. Uvarov, A. Vorobyev[†], Yu. Andreev,

A. Dermenev, S. Gninenko, N. Golubev, A. Karneyeu, D. Kirpichnikov, M. Kirsanov, N. Krasnikov, I. Tlisova, A. Toropin, T. Aushev, V. Gavrilov, N. Lychkovskaya, A. Nikitenko[97,98], V. Popov, A. Zhokin, M. Chadeeva[94], R. Chistov[94], S. Polikarpov[94], V. Andreev, M. Azarkin, M. Kirakosyan, A. Terkulov, E. Boos, V. Bunichev, M. Dubinin[83], L. Dudko, A. Ershov, A. Gribushin, V. Klyukhin, O. Kodolova[98], S. Obraztsov, S. Petrushanko, V. Savrin, A. Snigirev, V. Blinov[94], T. Dimova[94], A. Kozyrev[94], O. Radchenko[94], Y. Skovpen[94], V. Kachanov, D. Konstantinov, S. Slabospitskii, A. Uzunian, A. Babaev, V. Borshch, D. Druzhkin[99]

Authors affiliated with an institute or an international laboratory covered by a cooperation agreement with CERN

V. Chekhovsky, V. Makarenko

Authors affiliated with an institute formerly covered by a cooperation agreement with CERN

† Deceased.
1 Also at Yerevan State University, Yerevan, Armenia.
2 Also at TU Wien, Vienna, Austria.
3 Also at Ghent University, Ghent, Belgium.
4 Also at Universidade do Estado do Rio de Janeiro, Rio de Janeiro, Brazil.
5 Also at Universidade Estadual de Campinas, Campinas, Brazil.
6 Also at Federal University of Rio Grande do Sul, Porto Alegre, Brazil.
7 Also at UFMS, Nova Andradina, Brazil.
8 Also at University of Chinese Academy of Sciences, Beijing, China.
9 Also at China Center of Advanced Science and Technology, Beijing, China.
10 Also at University of Chinese Academy of Sciences, Beijing, China.
11 Also at China Spallation Neutron Source, Guangdong, China.
12 Now at Henan Normal University, Xinxiang, China.
13 Now at The University of Iowa, Iowa City, Iowa, USA.
14 Also at Université Libre de Bruxelles, Bruxelles, Belgium.
15 Also at an institute or an international laboratory covered by a cooperation agreement with CERN.
16 Also at Helwan University, Cairo, Egypt.
17 Now at Zewail City of Science and Technology, Zewail, Egypt.
18 Now at British University in Egypt, Cairo, Egypt.
19 Now at Cairo University, Cairo, Egypt.
20 Also at Purdue University, West Lafayette, Indiana, USA.
21 Also at Université de Haute Alsace, Mulhouse, France.
22 Also at Istinye University, Istanbul, Turkey.
23 Also at Tbilisi State University, Tbilisi, Georgia.
24 Also at The University of the State of Amazonas, Manaus, Brazil.
25 Also at University of Hamburg, Hamburg, Germany.
26 Also at RWTH Aachen University, III. Physikalisches Institut A, Aachen, Germany.
27 Also at Bergische University Wuppertal (BUW), Wuppertal, Germany.
28 Also at Brandenburg University of Technology, Cottbus, Germany.
29 Also at Forschungszentrum Jülich, Juelich, Germany.
30 Also at CERN, European Organization for Nuclear Research, Geneva, Switzerland.
31 Also at HUN-REN ATOMKI - Institute of Nuclear Research, Debrecen, Hungary.
32 Now at Universitatea Babes-Bolyai - Facultatea de Fizica, Cluj-Napoca, Romania.
33 Also at MTA-ELTE Lendület CMS Particle and Nuclear Physics Group, Eötvös Loránd University, Budapest, Hungary.
34 Also at HUN-REN Wigner Research Centre for Physics, Budapest, Hungary.
35 Also at Physics Department, Faculty of Science, Assiut University, Assiut, Egypt.
36 Also at Punjab Agricultural University, Ludhiana, India.
37 Also at University of Visva-Bharati, Santiniketan, India.
38 Also at Indian Institute of Science (IISc), Bangalore, India.
39 Also at IIT Bhubaneswar, Bhubaneswar, India.
40 Also at Institute of Physics, Bhubaneswar, India.
41 Also at University of Hyderabad, Hyderabad, India.
42 Also at Deutsches Elektronen-Synchrotron, Hamburg, Germany.
43 Also at Isfahan University of Technology, Isfahan, Iran.
44 Also at Sharif University of Technology, Tehran, Iran.
45 Also at Department of Physics, University of Science and Technology of Mazandaran, Behshahr, Iran.
46 Also at Department of Physics, Faculty of Science, Arak University, ARAK, Iran.
47 Also at Italian National Agency for New Technologies, Energy and Sustainable Economic Development, Bologna, Italy.
48 Also at Centro Siciliano di Fisica Nucleare e di Struttura Della Materia, Catania, Italy.
49 Also at Università degli Studi Guglielmo Marconi, Roma, Italy.
50 Also at Scuola Superiore Meridionale, Università di Napoli 'Federico II', Napoli, Italy.
51 Also at Fermi National Accelerator Laboratory, Batavia, Illinois, USA.
52 Also at Consiglio Nazionale delle Ricerche - Istituto Officina dei Materiali, Perugia, Italy.
53 Also at Department of Applied Physics, Faculty of Science and Technology, Universiti Kebangsaan Malaysia, Bangi, Malaysia.
54 Also at Consejo Nacional de Ciencia y Tecnología, Mexico City, Mexico.
55 Also at Trincomalee Campus, Eastern University, Sri Lanka, Nilaveli, Sri Lanka.
56 Also at Saegis Campus, Nugegoda, Sri Lanka.

[57] Also at National and Kapodistrian University of Athens, Athens, Greece.
[58] Also at Ecole Polytechnique Fédérale Lausanne, Lausanne, Switzerland.
[59] Also at University of Vienna, Vienna, Austria.
[60] Also at Universität Zürich, Zurich, Switzerland.
[61] Also at Stefan Meyer Institute for Subatomic Physics, Vienna, Austria.
[62] Also at Laboratoire d'Annecy-le-Vieux de Physique des Particules, IN2P3-CNRS, Annecy-le-Vieux, France.
[63] Also at Near East University, Research Center of Experimental Health Science, Mersin, Turkey.
[64] Also at Konya Technical University, Konya, Turkey.
[65] Also at Izmir Bakircay University, Izmir, Turkey.
[66] Also at Adiyaman University, Adiyaman, Turkey.
[67] Also at Bozok Universitetesi Rektörlügü, Yozgat, Turkey.
[68] Also at Marmara University, Istanbul, Turkey.
[69] Also at Milli Savunma University, Istanbul, Turkey.
[70] Also at Kafkas University, Kars, Turkey.
[71] Now at Istanbul Okan University, Istanbul, Turkey.
[72] Also at Hacettepe University, Ankara, Turkey.
[73] Also at Erzincan Binali Yildirim University, Erzincan, Turkey.
[74] Also at Istanbul University - Cerrahpasa, Faculty of Engineering, Istanbul, Turkey.
[75] Also at Yildiz Technical University, Istanbul, Turkey.
[76] Also at Vrije Universiteit Brussel, Brussel, Belgium.
[77] Also at School of Physics and Astronomy, University of Southampton, Southampton, United Kingdom.
[78] Also at IPPP Durham University, Durham, United Kingdom.
[79] Also at Monash University, Faculty of Science, Clayton, Australia.
[80] Also at Università di Torino, Torino, Italy.
[81] Also at Bethel University, St. Paul, Minnesota, USA.
[82] Also at Karamanoğlu Mehmetbey University, Karaman, Turkey.
[83] Also at California Institute of Technology, Pasadena, California, USA.
[84] Also at United States Naval Academy, Annapolis, Maryland, USA.
[85] Also at Ain Shams University, Cairo, Egypt.
[86] Also at Bingol University, Bingol, Turkey.
[87] Also at Georgian Technical University, Tbilisi, Georgia.
[88] Also at Sinop University, Sinop, Turkey.
[89] Also at Erciyes University, Kayseri, Turkey.
[90] Also at Horia Hulubei National Institute of Physics and Nuclear Engineering (IFIN-HH), Bucharest, Romania.
[91] Now at another institute or international laboratory covered by a cooperation agreement with CERN.
[92] Also at Texas A&M University at Qatar, Doha, Qatar.
[93] Also at Kyungpook National University, Daegu, Korea.
[94] Also at another institute or international laboratory covered by a cooperation agreement with CERN.
[95] Also at Institute of Nuclear Physics of the Uzbekistan Academy of Sciences, Tashkent, Uzbekistan.
[96] Also at Northeastern University, Boston, Massachusetts, USA.
[97] Also at Imperial College, London, United Kingdom.
[98] Now at Yerevan Physics Institute, Yerevan, Armenia.
[99] Also at Universiteit Antwerpen, Antwerpen, Belgium.